

Supplementary information for:

Structural variation of types IV-A1- and IV-A3-mediated CRISPR interference

Čepaitė, R.¹, Klein, N.², Mikšys, A.^{1,3}, Camara-Wilpert, S.⁴, Ragožius, V.¹, Benz, F.^{5,6}, Skorupskaitė A.¹, Becker, H.², Žvejytė, G.¹, Steube, N.⁷, Hochberg, G.K.A.^{7,8,9}, Randau, L.^{2,9}, Pinilla-Redondo, R.⁴, Malinauskaitė, L.^{*1,10}, Pausch, P.^{*1}

¹ LSC-EMBL Partnership Institute for Genome Editing Technologies, Life Sciences Center, Vilnius University, Saulėtekio al. 7, 10257 Vilnius, Lithuania

² Department of Biology, Philipps-Universität Marburg, Hans-Meerwein-Straße 6, D-35032, Marburg, Germany

³ Current: ATEM Structural Discovery GmbH, Büchelstraße 54, 42855 Remscheid, Germany

⁴ Department of Biology, Section of Microbiology, University of Copenhagen, Universitetsparken 15, 2100 Copenhagen, Denmark

⁵ Institut Pasteur, Université Paris Cité, CNRS UMR6047, 75015 Paris, Synthetic Biology, Paris 75015, France

⁶ Institut Pasteur, Université Paris Cité, CNRS UMR3525, Microbial Evolutionary Genomics, Paris 75015, France

⁷ Evolutionary Biochemistry Group, Max Planck Institute for Terrestrial Microbiology, Karl-von-Frisch-Straße 10, D-35043, Marburg, Germany

⁸ Department of Chemistry, Philipps-Universität Marburg, Hans-Meerwein-Straße 4, D-35032, Marburg, Germany

⁹ Center for Synthetic Microbiology (SYNMIKRO), Karl-von-Frisch-Straße 14, 35043 Marburg, Germany

¹⁰ Current: BioNTech UK Ltd, Cambridge Biomedical Campus, Francis Crick Ave, Trumpington, Cambridge CB2 0QH, UK

Correspondence and requests for materials should be addressed to L.M. (email: lina.malinauskaite@biontech.co.uk) and P.P. (email: patrick.pausch@gmc.vu.lt).

Content:

Supplementary Tables 1-4	(p. 2-10)
Supplementary Figures 1-21	(p. 11-34)
Supplementary References	(p. 35)
Supplementary Source Data	(p. 36-61)

SUPPLEMENTARY TABLES

Supplementary Tab. 1 | Cryo-EM data collection, refinement and validation statistics for type IV-A1 in absence and presence of DinG, and type IV-A3 in absence of DinG.

	Type IV-A1 in complex with DNA (EMD-19046 , EMD-19120 , EMD-19124 , PDB-ID: 8RC3)	Type IV-A1 in complex with DNA and DinG (EMD-19125 , EMD-19126 , EMD-19127 , EMD-51026 , PDB-ID: 8REI)	Type IV-A3 in complex with DNA (EMD-19045 , PDB-ID: 8RC2)
Data collection and processing			
Magnification	×92000		×92000
Voltage (kV)	200		200
Exposure (e ⁻ /Å ²)	30		30
Defocus range (μm)	-2.0 to -1.0		-2.0 to -1.0
Pixel size (Å)	1.1		1.1
Initial particles	1,022,768		1,082,094
Final particles	103,699	55,924	104,035
Symmetry imposed	C1	C1	C1
Resolution (Å)	2.96	3.18	3.1
FSC cutoff	0.143	0.143	0.143
Map resolution range (Å)	2.5-7	3-8	2.5-7
Refinement			
Model resolution (Å)	3.1	3.7	3.3
0.143 FSC Threshold (Å)	2.0	2.2	2.8
Map sharpening <i>B</i> factor	96.7	81.3	70
Model composition			
Non-hydrogen atoms	19897	24687	19755
Protein residues	2297	2877	2304
Nucleotides	112	129	94
Ligands	ZN: 1	ZN: 1	ZN: 1
<i>B</i> factors (Å ²)			
Protein	67.55	113.57	124.34
Nucleotide	102.27	125.16	132.81
Ligand	92.18	104.23	166.56
Validation			
Bonds (r.m.s. deviations)			
Length (Å) (# > 4s)	0.004 (0)	0.003 (0)	0.006 (0)
Angles (°) (# > 4s)	0.556 (3)	0.544 (1)	0.614 (0)
MolProbity score	1.59	1.57	1.41
Clash score	10.06	10.20	7.49
Poor rotamers (%)	0	0	0.42
Ramachandran plot (%)			

Outliers	0.00	0.00	0.00
Allowed	2.29	2.08	1.32
Favored	97.71	97.92	98.68
Rama-Z score, whole (r.m.s. Rama-Z)	0.49 (0.17)	0.80 (0.16)	0.85 (0.17)
CC (mask)	0.86	0.81	0.82
CC (box)	0.86	0.89	0.73

Supplementary Tab. 2 | Cryo-EM data collection, refinement and validation statistics for type IV-A3 in presence of DinG.

	Type IV-A3 in complex with DNA and DinG (state I) (EMD-19688 , PDB-ID: 8S35)	Type IV-A3 in complex with DNA and DinG (state II) (EMD-19689 , PDB-ID: 8S36)	Type IV-A3 in complex with DNA and DinG (state III) (EMD-19690 , PDB-ID: 8S37)
Data collection and processing			
Magnification	×92000		
Voltage (kV)	200		
Exposure (e ⁻ /Å ²)	30.31		
Defocus range (µm)	-2.0 to -1.0		
Pixel size (Å)	1.1		
Initial particles	4,069,893		
Final particles	45,309	48,197	46,284
Symmetry imposed	C1	C1	C1
Resolution (Å)	2.90	2.88	2.89
FSC cutoff	0.143	0.143	0.143
Map resolution range (Å)	2.5-7	2.5-7	2.5-7
Refinement			
Model resolution (Å)	3.6	3.7	3.6
0.143 FSC Threshold (Å)	3.0	3.0	3.0
Map sharpening <i>B</i> factor	71.1	72.6	71.9
Model composition			
Non-hydrogen atoms	25082	24249	25085
Protein residues	2936	2838	2947
Nucleotides	112	108	107
Ligands	ZN: 1	ZN: 1	ZN: 1
<i>B</i> factors (Å ²)			
Protein	204.28	203.73	221.25
Nucleotide	198.85	204.32	205.08
Ligand	215.96	217.23	192.95
Validation			
Bonds (r.m.s. deviations)			
Length (Å) (# > 4s)	0.004 (0)	0.004 (0)	0.004 (0)
Angles (°) (# > 4s)	0.726 (10)	0.728 (7)	0.659 (1)

MolProbity score	1.51	1.52	1.48
Clash score	9.69	10.07	9.09
Poor rotamers (%)	0.41	0.81	0.90
Ramachandran plot (%)			
Outliers	0.00	0.07	0.14
Allowed	0.28	0.50	0.31
Favored	99.72	99.43	99.55
Rama-Z score, whole (r.m.s. Rama-Z)	-0.29 (0.15)	-1.16 (0.15)	-1.05 (0.15)
CC (mask)	0.82	0.81	0.82
CC (box)	0.90	0.89	0.89

Supplementary Tab. 3 | DNA oligonucleotides.

Sequence name	Purpose	Sequence (5' → 3')
Type IV-A1 target strand	cryo-EM sample reconstitution	HO-CGGTCGGGTCATACGTCGCGTCTCGAATCTGATGCGTAACTTG GATGCTTCGTGCGTGATG
Type IV-A1 non-target strand	cryo-EM sample reconstitution	HO-CATCACGCACGAAGACCAAGTCAATGCTTAGTCTAATACCTGC GCTCGTATGACCCGACCG
Type IV-A3 target strand	cryo-EM sample reconstitution	HO-CCCTCCCTCCAGCTTCCGAGACCCTTCGGGAGGTGCATCCCGG TCTCGCTTGGCCTCCTC
Type IV-A3 non-target strand	cryo-EM sample reconstitution	HO-GAGGAGGCCAAGATCTCAATTCGTACAAGAAATCCTTTGAG ATGAAGCTGGAGGGAGGG
EMSA probe forward primer	EMSA probe amplification	CTATCCCATATCACCAGCTCAC
EMSA probe reverse primer	EMSA probe amplification	ATTO647N-GTTGATCGGCACGTAAGAG

Supplementary Tab. 4 | Plasmids.*

ID	Purpose	Features	Selection marker
pRC002 Ref. ¹	Protein purification	pRSF-Duet1 derived plasmid containing type IV-A3 genes with C-terminally hexa-histidine tagged <i>csf2</i> (<i>cas7</i>)	Kanamycin
pRC004 Ref. ¹	Protein purification	pYTK095 derived plasmid containing a repeat-spacer-repeat motif from type IV-A3 CRISPR-array. Contains non-targeting BsaI-GG stuffer spacer.	Ampicillin
pNK25	Protein purification	pRSF-Duet1 derived plasmid containing type IV-A1 genes with C-terminally hexa-histidine tagged <i>csf1</i> (<i>cas8</i>) in MCS1 and <i>dinG</i> in MCS2	Kanamycin
pAG33	Protein purification	pUC19 derived plasmid containing a repeat-spacer-repeat motif from type IV-A1 CRISPR-array.	Ampicillin
pNK27	Protein purification	pRSF-Duet1 derived plasmid containing type IV-A1 genes with C-terminally hexa-histidine tagged <i>csf1</i> (<i>cas8</i>) in MCS1	Kanamycin

pAG19	Protein purification	pET20b derived plasmid with C-terminally hexa-histidine tagged <i>dinG</i>	Ampicillin
pSR77	Repression assay	pRSFDuet-1 derived plasmid containing type IV-A1 genes and a repeat-spacer-repeat mini-CRISPR (non-targeting control)	Kanamycin
pSR102	Repression assay	pRSFDuet-1 derived plasmid containing type IV-A1 genes and a repeat-spacer-repeat mini-CRISPR targeting <i>lacZ</i> (targeting control)	Kanamycin
pNK92	Repression assay	pRSFDuet-1 derived plasmid encoding DinG with amino acid substitution R440A and a repeat-spacer-repeat motif targeting <i>lacZ</i>	Kanamycin
pNK93	Repression assay	pRSFDuet-1 derived plasmid encoding DinG with amino acid substitution W494A and a repeat-spacer-repeat motif targeting <i>lacZ</i>	Kanamycin
pNK94	Repression assay	pRSFDuet-1 derived plasmid encoding DinG with amino acid substitution K661A and a repeat-spacer-repeat motif targeting <i>lacZ</i>	Kanamycin
pNK95	Repression assay	pRSFDuet-1 derived plasmid encoding DinG with amino acid substitution R493A and a repeat-spacer-repeat motif targeting <i>lacZ</i>	Kanamycin
pNK96	Repression assay	pRSFDuet-1 derived plasmid encoding DinG with amino acid substitution Q390A and a repeat-spacer-repeat motif targeting <i>lacZ</i>	Kanamycin
pNK97	Repression assay	pRSFDuet-1 derived plasmid encoding DinG with amino acid substitution K463A and a repeat-spacer-repeat motif targeting <i>lacZ</i>	Kanamycin
pNK98	Repression assay	pRSFDuet-1 derived plasmid encoding DinG with amino acid substitution I567W and a repeat-spacer-repeat motif targeting <i>lacZ</i>	Kanamycin
pNK99	Repression assay	pRSFDuet-1 derived plasmid encoding DinG with amino acid substitution R653A and a repeat-spacer-repeat motif targeting <i>lacZ</i>	Kanamycin
pNK100	Protein purification	pET20b derived plasmid encoding DinG with amino acid substitution R440A	Ampicillin
pNK101	Protein purification	pET20b derived plasmid encoding DinG with amino acid substitution W494A	Ampicillin
pNK102	Protein purification	pET20b derived plasmid encoding DinG with amino acid substitution R653A	Ampicillin
pNK112	Repression assay	pYTK095 derived plasmid containing a repeat-spacer-repeat mini-CRISPR from type IV-A3 CRISPR-array with a spacer targeting <i>lacZ</i> .	Ampicillin
pNK113	Repression assay	pRSF-Duet1 derived plasmid containing type IV-A3 genes and encoding DinG with a truncated C-terminus (Δ 617-624)	Kanamycin
pNK114	Repression assay	pRSF-Duet1 derived plasmid containing type IV-A3 genes and encoding DinG with amino acid substitution Y527W	Kanamycin
pNK115	Repression assay	pRSF-Duet1 derived plasmid containing type IV-A3 genes and encoding DinG with amino acid substitutions R537A, T538W and F539A	Kanamycin
pNK117	Repression assay	pRSF-Duet1 derived plasmid containing type IV-A3 genes and encoding DinG with amino acid substitution L588W	Kanamycin

pNK118	Repression assay	pRSF-Duet1 derived plasmid containing type IV-A3 genes and encoding DinG with amino acid substitution Y527A	Kanamycin
pNK119	Repression assay	pRSF-Duet1 derived plasmid containing type IV-A3 genes and encoding DinG with amino acid substitution R544A	Kanamycin
pNK121	Repression assay	pRSF-Duet1 derived plasmid containing type IV-A3 genes and encoding DinG with amino acid substitutions R605A and R608A	Kanamycin
pNK122	Repression assay	pRSF-Duet1 derived plasmid containing type IV-A3 genes and encoding DinG with amino acid substitution K288A	Kanamycin
pNK125	Repression assay	pRSF-Duet1 derived plasmid containing type IV-A3 genes and encoding DinG with amino acid substitution L588A	Kanamycin
pNK126	Protein purification	pRSF-Duet1 derived plasmid encoding DinG with amino acid substitution Y527A	Kanamycin
pNK127	Protein purification	pRSF-Duet1 derived plasmid encoding DinG with amino acid substitutions R537A, T538W and F539A	Kanamycin
pNK128	Repression assay	pRSF-Duet1 derived plasmid containing type IV-A3 genes and encoding DinG with amino acid substitutions N412A, I418A and Q422A	Kanamycin
pSR24	Mismatch tolerance assays in <i>E. coli</i>	pCDFDuet-1 derived plasmid containing a repeat-spacer-repeat mini-CRISPR from type IV-A1 CRISPR array with no mutations (no mismatch control)	Spectinomycin
pHB01	Mismatch tolerance assays in <i>E. coli</i>	pCDFDuet-1 derived plasmid containing a repeat-spacer-repeat mini-CRISPR from type IV-A1 CRISPR array with spacer mutation in position 1 (C1G)	Spectinomycin
pHB02	Mismatch tolerance assays in <i>E. coli</i>	pCDFDuet-1 derived plasmid containing a repeat-spacer-repeat mini-CRISPR from type IV-A1 CRISPR array with spacer mutations in positions 2,3,4 (A2T, T3A, C4G)	Spectinomycin
pHB03	Mismatch tolerance assays in <i>E. coli</i>	pCDFDuet-1 derived plasmid containing a repeat-spacer-repeat mini-CRISPR from type IV-A1 CRISPR array with spacer mutation in position 5 (C5G)	Spectinomycin
pHB04	Mismatch tolerance assays in <i>E. coli</i>	pCDFDuet-1 derived plasmid containing a repeat-spacer-repeat mini-CRISPR from type IV-A1 CRISPR array with spacer mutation in position 6 (A6G)	Spectinomycin
pHB05	Mismatch tolerance assays in <i>E. coli</i>	pCDFDuet-1 derived plasmid containing a repeat-spacer-repeat mini-CRISPR from type IV-A1 CRISPR array with spacer mutation in position 7 (A7T)	Spectinomycin
pHB06	Mismatch tolerance assays in <i>E. coli</i>	pCDFDuet-1 derived plasmid containing a repeat-spacer-repeat mini-CRISPR from type IV-A1 CRISPR array with spacer mutation in position 8 (G8C)	Spectinomycin
pNK50	Mismatch tolerance assays in <i>E. coli</i>	pCDFDuet-1 derived plasmid containing a repeat-spacer-repeat mini-CRISPR from type IV-A1 CRISPR array with spacer mutation in position 4 (C4G)	Spectinomycin
pNK71	Mismatch tolerance assays in <i>E. coli</i>	pCDFDuet-1 derived plasmid containing a repeat-spacer-repeat mini-CRISPR from type IV-A1 CRISPR array with spacer mutation in position 2 (A2T)	Spectinomycin
pNK72	Mismatch tolerance assays in <i>E. coli</i>	pCDFDuet-1 derived plasmid containing a repeat-spacer-repeat mini-CRISPR from type IV-A1 CRISPR array with spacer mutation in position 3 (T3A)	Spectinomycin

pNK59	Mismatch tolerance assays in <i>E. coli</i>	pCDFDuet-1 derived plasmid containing a repeat-spacer-repeat mini-CRISPR from type IV-A1 CRISPR array with spacer mutation in position 9 (T9A)	Spectinomycin
pNK60	Mismatch tolerance assays in <i>E. coli</i>	pCDFDuet-1 derived plasmid containing a repeat-spacer-repeat mini-CRISPR from type IV-A1 CRISPR array with spacer mutation in position 10 (T10A)	Spectinomycin
pNK61	Mismatch tolerance assays in <i>E. coli</i>	pCDFDuet-1 derived plasmid containing a repeat-spacer-repeat mini-CRISPR from type IV-A1 CRISPR array with spacer mutation in position 11 (A11T)	Spectinomycin
pNK62	Mismatch tolerance assays in <i>E. coli</i>	pCDFDuet-1 derived plasmid containing a repeat-spacer-repeat mini-CRISPR from type IV-A1 CRISPR array with spacer mutation in position 1 (C12G)	Spectinomycin
pNK63	Mismatch tolerance assays in <i>E. coli</i>	pCDFDuet-1 derived plasmid containing a repeat-spacer-repeat mini-CRISPR from type IV-A1 CRISPR array with spacer mutation in position 13 (G13C)	Spectinomycin
pNK64	Mismatch tolerance assays in <i>E. coli</i>	pCDFDuet-1 derived plasmid containing a repeat-spacer-repeat mini-CRISPR from type IV-A1 CRISPR array with spacer mutation in position 14 (C14G)	Spectinomycin
pNK65	Mismatch tolerance assays in <i>E. coli</i>	pCDFDuet-1 derived plasmid containing a repeat-spacer-repeat mini-CRISPR from type IV-A1 CRISPR array with spacer mutation in position 15 (A15T)	Spectinomycin
pNK66	Mismatch tolerance assays in <i>E. coli</i>	pCDFDuet-1 derived plasmid containing a repeat-spacer-repeat mini-CRISPR from type IV-A1 CRISPR array with spacer mutation in position 16 (T16A)	Spectinomycin
pNK67	Mismatch tolerance assays in <i>E. coli</i>	pCDFDuet-1 derived plasmid containing a repeat-spacer-repeat mini-CRISPR from type IV-A1 CRISPR array with spacer mutations in positions 17-20 (CAGA→GTCT)	Spectinomycin
pNK68	Mismatch tolerance assays in <i>E. coli</i>	pCDFDuet-1 derived plasmid containing a repeat-spacer-repeat mini-CRISPR from type IV-A1 CRISPR array with spacer mutations in positions 21-24 (TTCG→AAGC)	Spectinomycin
pNK69	Mismatch tolerance assays in <i>E. coli</i>	pCDFDuet-1 derived plasmid containing a repeat-spacer-repeat mini-CRISPR from type IV-A1 CRISPR array with spacer mutations in positions 25-28 (AGAC→TCTG)	Spectinomycin
pNK70	Mismatch tolerance assays in <i>E. coli</i>	pCDFDuet-1 derived plasmid containing a repeat-spacer-repeat mini-CRISPR from type IV-A1 CRISPR array with spacer mutations in positions 29-32 (GCGA→CGCT)	Spectinomycin
pSR14	Mismatch tolerance assays in <i>E. coli</i>	pACYCDuet-1 derived plasmid containing a type IV-A1 target sequence	Chloramphenicol
pSR15	Mismatch tolerance assays in <i>E. coli</i>	pACYCDuet-1 derived plasmid containing a non-target sequence	Chloramphenicol
pHB07	Mismatch tolerance assays in <i>E. coli</i>	pACYCDuet-1 derived plasmid containing a type IV-A1 protospacer with mutation in position 1 (G1C)	Chloramphenicol
pHB08	Mismatch tolerance assays in <i>E. coli</i>	pACYCDuet-1 derived plasmid containing a type IV-A1 protospacer with mutation in position 2 (T2A)	Chloramphenicol
pHB09	Mismatch tolerance assays in <i>E. coli</i>	pACYCDuet-1 derived plasmid containing a type IV-A1 protospacer with mutation in position 3 (A3T)	Chloramphenicol

pHB10	Mismatch tolerance assays in <i>E. coli</i>	pACYCDuet-1 derived plasmid containing a type IV-A1 protospacer with mutation in position 4 (G4C)	Chloramphenicol
pHB11	Mismatch tolerance assays in <i>E. coli</i>	pACYCDuet-1 derived plasmid containing a type IV-A1 protospacer with mutation in position 5 (G5C)	Chloramphenicol
pHB12	Mismatch tolerance assays in <i>E. coli</i>	pACYCDuet-1 derived plasmid containing a type IV-A1 protospacer with mutation in position 6 (T6A)	Chloramphenicol
pHB13	Mismatch tolerance assays in <i>E. coli</i>	pACYCDuet-1 derived plasmid containing a type IV-A1 protospacer with mutation in position 7 (T7A)	Chloramphenicol
pHB14	Mismatch tolerance assays in <i>E. coli</i>	pACYCDuet-1 derived plasmid containing a type IV-A1 protospacer with mutation in position 8 (C8G)	Chloramphenicol
pHB15	Mismatch tolerance assays in <i>E. coli</i>	pACYCDuet-1 derived plasmid containing a type IV-A1 protospacer with mutations in position 2,3,4 (T2A, A3T, G4C)	Chloramphenicol
pNK82	Mismatch tolerance assays in <i>P. oleovorans</i>	pSR106 derived plasmid containing a repeat-spacer-repeat motif from type IV-A1 with a spacer mutation in position 1 (G1C)	Spectinomycin
pNK83	Mismatch tolerance assays in <i>P. oleovorans</i>	pSR106 derived plasmid containing a repeat-spacer-repeat motif from type IV-A1 with a spacer mutation in position 2 (T2A)	Spectinomycin
pNK84	Mismatch tolerance assays in <i>P. oleovorans</i>	pSR106 derived plasmid containing a repeat-spacer-repeat motif from type IV-A1 with a spacer mutation in position 3 (G3C)	Spectinomycin
pNK85	Mismatch tolerance assays in <i>P. oleovorans</i>	pSR106 derived plasmid containing a repeat-spacer-repeat motif from type IV-A1 with a spacer mutation in position 4 (A4T)	Spectinomycin
pNK86	Mismatch tolerance assays in <i>P. oleovorans</i>	pSR106 derived plasmid containing a repeat-spacer-repeat motif from type IV-A1 with a spacer mutation in position 5 (T5A)	Spectinomycin
pNK87	Mismatch tolerance assays in <i>P. oleovorans</i>	pSR106 derived plasmid containing a repeat-spacer-repeat motif from type IV-A1 with a spacer mutation in position 6 (G6C)	Spectinomycin
pNK88	Mismatch tolerance assays in <i>P. oleovorans</i>	pSR106 derived plasmid containing a repeat-spacer-repeat motif from type IV-A1 with a spacer mutation in position 7 (C7G)	Spectinomycin
pNK89	Mismatch tolerance assays in <i>P. oleovorans</i>	pSR106 derived plasmid containing a repeat-spacer-repeat motif from type IV-A1 with a spacer mutation in position 8 (G8C)	Spectinomycin
pNK91	Mismatch tolerance assays in <i>P. oleovorans</i>	pSR106 derived plasmid containing a repeat-spacer-repeat mini-CRISPR from type IV-A1 (no mismatch control)	Spectinomycin
pSR106	Mismatch tolerance assays in <i>P. oleovorans</i>	pSEVA424 derived plasmid containing a repeat-spacer-repeat mini-CRISPR from type IV-A1 (non-targeting control)	Spectinomycin
pRC040	Mismatch tolerance assays <i>in vitro</i>	pRSF-Duet1 derived plasmid containing type IV-A3 genes with C-terminally hexa-histidine tagged <i>csf2</i> (<i>cas7</i>) with a Δ 191-208 (GSSG) mutation	Kanamycin

pRC041	Mismatch tolerance assays <i>in vitro</i>	pRSF-Duet1 derived plasmid containing type IV-A3 genes with C-terminally hexa-histidine tagged <i>csf2 (cas7)</i> with a $\Delta 184-216$ (GSSG) mutation	Kanamycin
pRC042	Mismatch tolerance assays <i>in vitro</i>	pRSF-Duet1 derived plasmid containing type IV-A3 genes with C-terminally hexa-histidine tagged <i>csf2 (cas7)</i> with a $\Delta 177-224$ (GSSG) mutation	Kanamycin
pRC043	Mismatch tolerance assays <i>in vitro</i>	pACYCDuet-1 derived plasmid containing a protospacer mutation in positions 13-17	Chloramphenicol
pRC044	Mismatch tolerance assays <i>in vitro</i>	pACYCDuet-1 derived plasmid containing a protospacer mutation in positions 17-20	Chloramphenicol
pRC045	Mismatch tolerance assays <i>in vitro</i>	pACYCDuet-1 derived plasmid containing a protospacer mutation in positions 19-23	Chloramphenicol
pRC046	Mismatch tolerance assays <i>in vitro</i>	pACYCDuet-1 derived plasmid containing a protospacer mutation in positions 21-24	Chloramphenicol
pRC047	Mismatch tolerance assays <i>in vitro</i>	pACYCDuet-1 derived plasmid containing a protospacer mutation in position 25-28	Chloramphenicol
pRC048	Mismatch tolerance assays <i>in vitro</i>	pACYCDuet-1 derived plasmid containing a protospacer mutation in position 25-29	Chloramphenicol
pRC049	Mismatch tolerance assays <i>in vitro</i>	pACYCDuet-1 derived plasmid containing a protospacer mutation in position 31-32	Chloramphenicol
pSJK35	Phage targeting assays	pHERD30T derived plasmid containing repeat-spacer-repeat mini-CRISPR from type IV-A3 CRISPR-array with a spacer targeting <i>phage λ-vir</i>	Gentamicin
pSC179	Phage targeting assays	pHERD30T derived plasmid containing containing a non-target sequence	Gentamicin
pSC031	Phage targeting assays	pMMB-67-HE derived plasmid containing type IV-A3 genes	Ampicillin
pSC289	Phage targeting assays	pMMB-67-HE derived plasmid containing type IV-A3 genes and encoding Cas7 with amino acid substitution W119A	Ampicillin
pSC290	Phage targeting assays	pMMB-67-HE derived plasmid containing type IV-A3 genes and encoding Cas7 with amino acid substitution F95A	Ampicillin
pSC291	Phage targeting assays	pMMB-67-HE derived plasmid containing type IV-A3 genes and encoding Cas8 with amino acid substitution K155A	Ampicillin
pSC292	Phage targeting assays	pMMB-67-HE derived plasmid containing type IV-A3 genes and encoding Cas5 with amino acid substitution K119A	Ampicillin
pSC293	Phage targeting assays	pMMB-67-HE derived plasmid containing type IV-A3 genes and encoding Cas5 with amino acid substitution R120A	Ampicillin
pSC294	Phage targeting assays	pMMB-67-HE derived plasmid containing type IV-A3 genes and encoding Cas5 with amino acid substitution R121A	Ampicillin
pSC295	Phage targeting assays	pMMB-67-HE derived plasmid containing type IV-A3 genes and encoding Cas8 with amino acid substitution V154A	Ampicillin

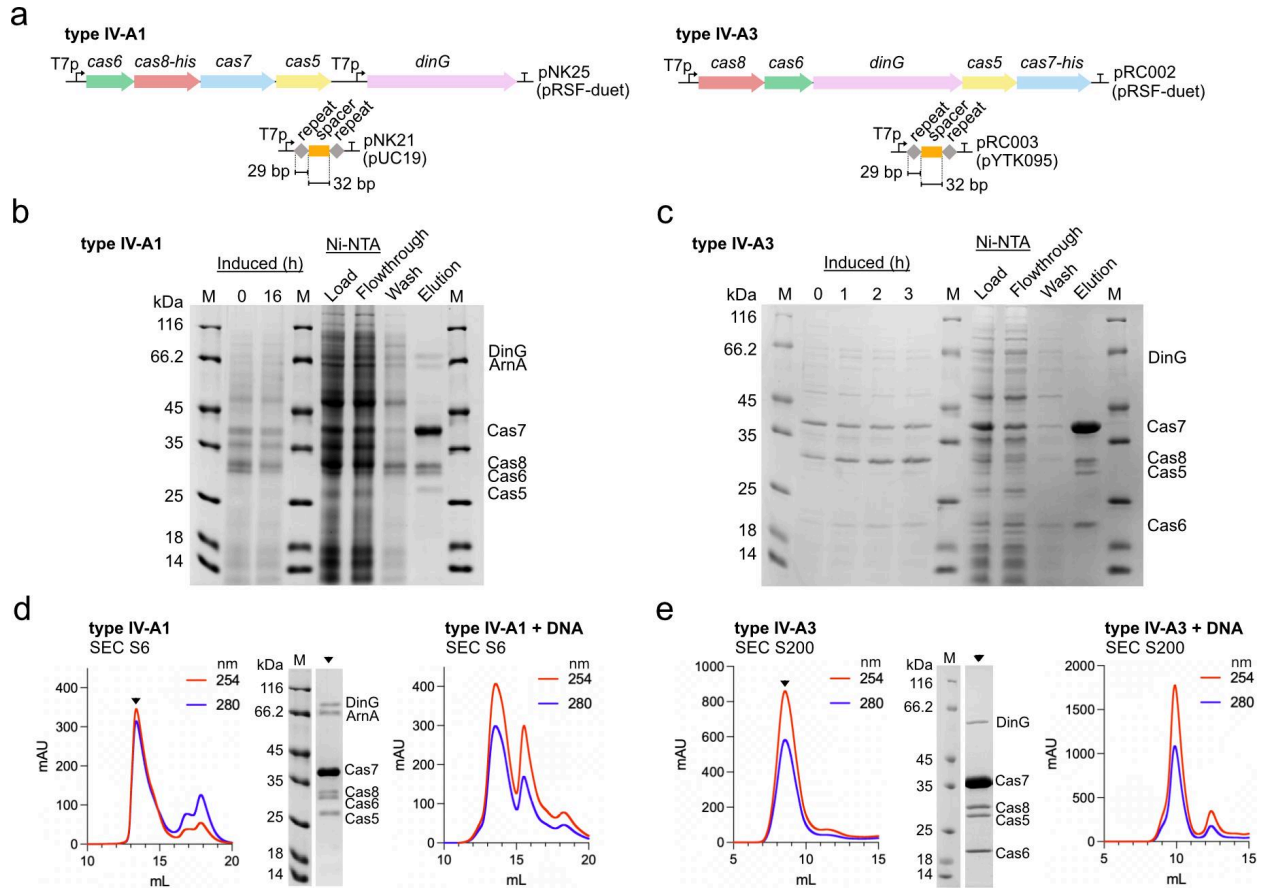
pSC296	Phage targeting assays	pMMB-67-HE derived plasmid containing type IV-A3 genes and encoding Cas5 with amino acid substitution T114A	Ampicillin
pSC297	Phage targeting assays	pMMB-67-HE derived plasmid containing type IV-A3 genes and encoding Cas5 with amino acid substitution L112A	Ampicillin
pSC298	Phage targeting assays	pMMB-67-HE derived plasmid containing type IV-A3 genes and encoding Cas8 with amino acid substitution K79A	Ampicillin
pSC299	Phage targeting assays	pMMB-67-HE derived plasmid containing type IV-A3 genes and encoding Cas8 with amino acid substitution Y51A	Ampicillin
pSC300	Phage targeting assays	pMMB-67-HE derived plasmid containing type IV-A3 genes and encoding Cas5 with amino acid substitutions R102A, R104A, R105A, R110A	Ampicillin

* plasmid sequences are provided as: Supplementary Data 2. Plasmid Sequences.

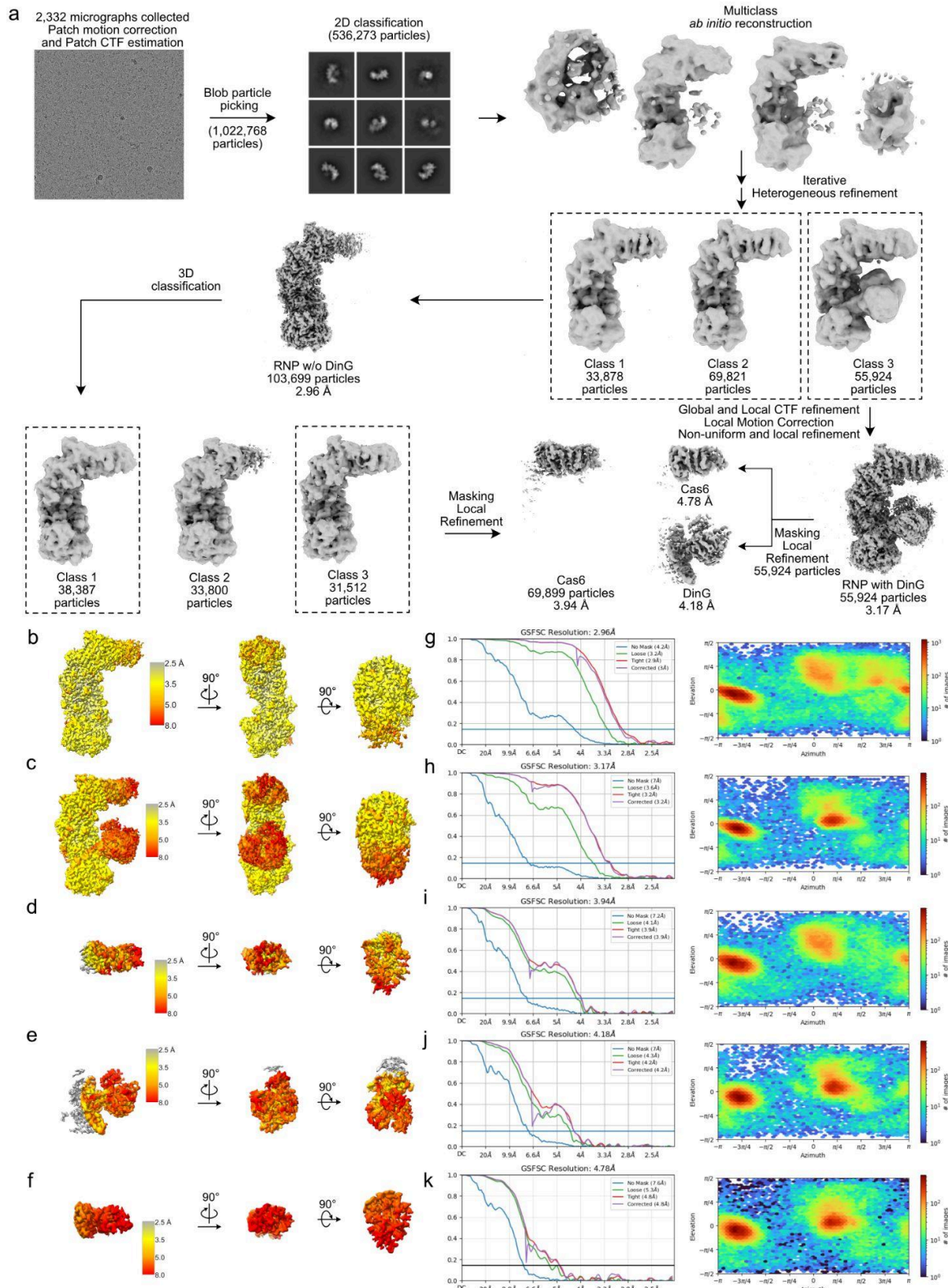
Supplementary Tab. 5 | Bacterial strains.

Strain	Genotype	Purpose
<i>E. coli</i> Mach1	<i>F-</i> $\phi 80(lacZ)\Delta M15 \Delta lacX74 hsdR(rK-mK+) \Delta recA1398 endA1 tonA$	Cloning
<i>E. coli</i> BL21 Star (DE3)	<i>F-</i> <i>ompT hsdSB (rB-mB-) gal dcm rne131 (DE3)</i>	Expression
<i>E. coli</i> DH5 α	<i>F-</i> <i>endA1, glnV44, thi-1, recA1, relA1, gyrA96, deoR, nupG, purB20, $\phi 80dlacZ\Delta M15 \Delta(lacZYA-argF), U169, hsdR17(rK-mK+), \lambda-$</i>	Cloning
<i>E. coli</i> BL21(DE3) LOBSTR	<i>F-</i> <i>ompT gal dcm lon hsdSB(rB-mB-) λ (DE3) [lacI lacUV5-T7p07 ind1 sam7 nin5] [malB⁺]K-12(λS)</i>	Expression
<i>E. coli</i> BL21-AI	<i>F-</i> <i>ompT gal dcm lon hsdSB(rB-mB-) [malB⁺]K-12(λS) araB::T7RNAP-tetA</i>	EOT, repression assays and expression
<i>P. oleovorans</i> DSM1045	wild type	Reporter gene assays
<i>E. coli</i> WM3064	<i>thrB1004 pro thi rpsL hsdS lacZ\Delta M15 RP4-1360 $\Delta(araBAD)567 \Delta dapA1341::[erm pir]$</i>	Conjugation
<i>E. coli</i> GeneHogs	<i>F-</i> <i>mcrA $\Delta(mrr-hsdRMS-mcrBC) \phi 80lacZ\Delta M15 \Delta lacX74 recA1 araD139 \Delta(araleu)7697 galU galK rpsL (StrR) endA1 nupG fhuA::IS2$ (confers phage T1 resistance)</i>	Cloning, phage targeting assays

SUPPLEMENTARY FIGURES

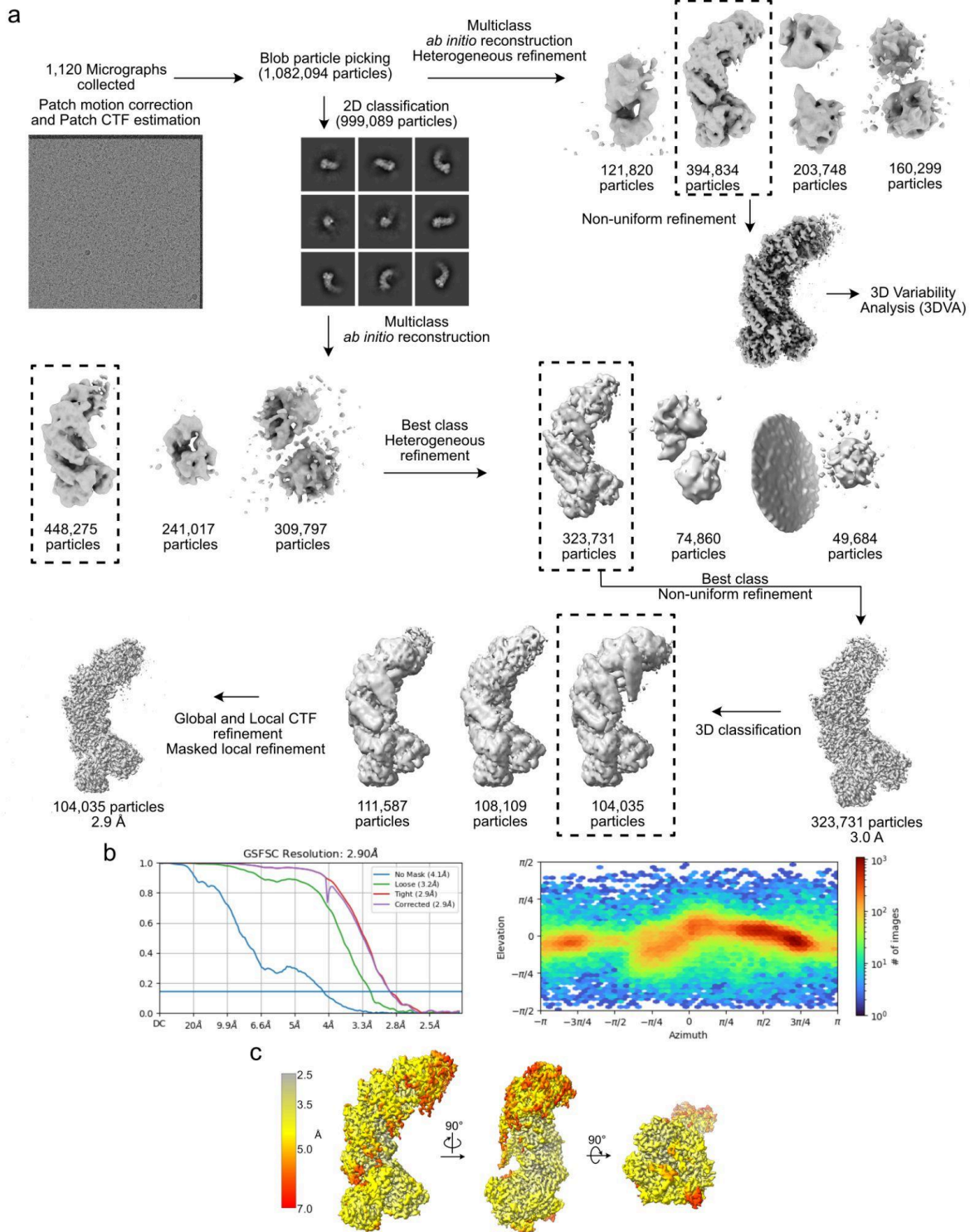


Supplementary Fig. 1 | Reconstitution of DNA-bound type IV-A RNP complexes. **a** Scheme illustrating type IV-A expression plasmids. **b** and **c**, SDS-PAGE of types IV-A1 (**b**) and IV-A3 (**c**) effector complex expression and Ni-NTA affinity chromatography samples. **d** SEC traces (S6 10/300) of binary (left) and DNA-bound ternary (right) type IV-A1 effector complexes. **e** SEC traces (S200 10/300) of binary (left) and DNA-bound ternary (right) type IV-A3 effector complexes.

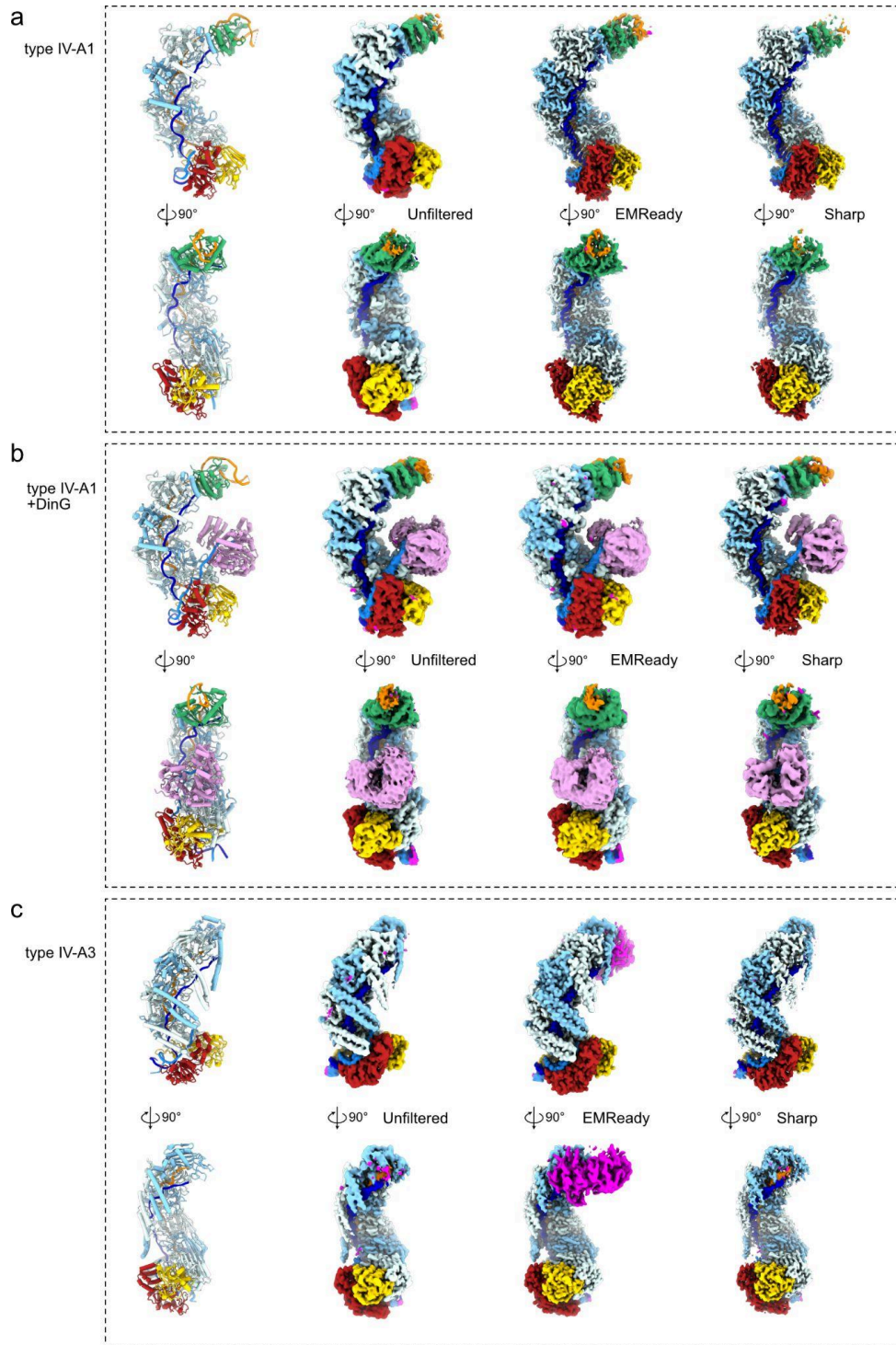


Supplementary Fig. 2 | Cryo-EM data processing for type IV-A1 in complex with DNA. a Processing workflow of the type IV-A1 dataset. All steps were performed in CryoSPARC (v. 4.2), except

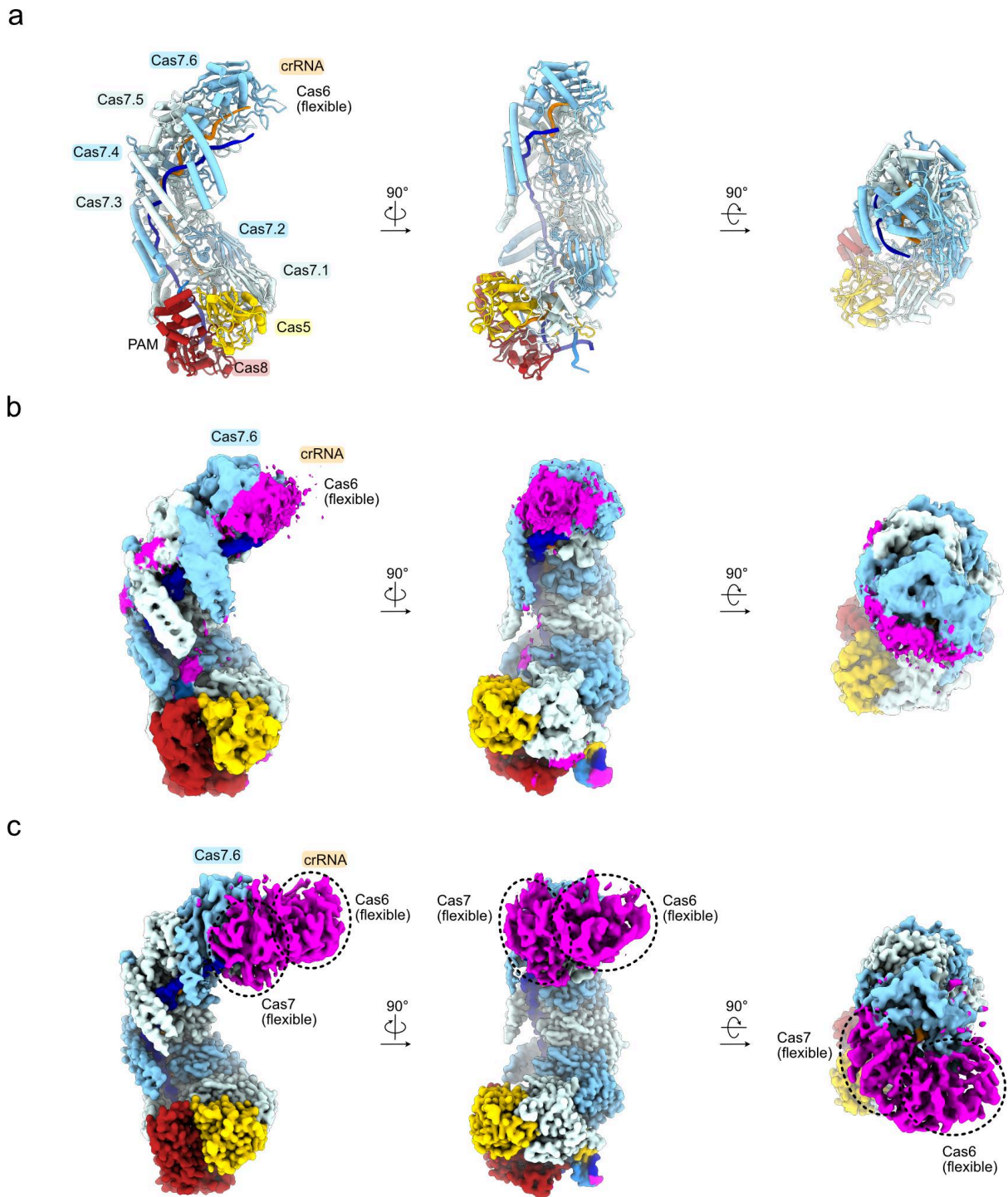
for refinement of Cas6 in the DinG bound state (**f**, **k**), which was performed in CryoSPARC (v4.5). **b** and **c** Local resolution map, calculated in CryoSPARC (v. 4.2) for the type IV-A1 complex in the absence of DinG (**b**) and presence of DinG (**c**). **d-f** Local resolution focused maps of Cas6 (**d**), DinG (**f**) and Cas6 of the DinG bound complex (**f**). **g-k**, FSC curves and angular distribution plots calculated in CryoSPARC (v. 4.2 and 4.5) for type IV-A1 complex in absence of DinG (**g**), the focused map of Cas6 (**i**); the type IV-A1 complex with DinG bound (**h**), the focused maps of DinG (**j**), and Cas6 (**k**). The global resolution at FSC 0.143 is indicated by a solid blue line.



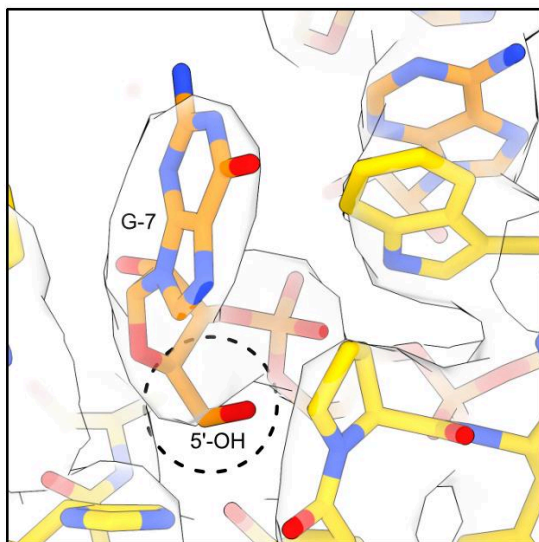
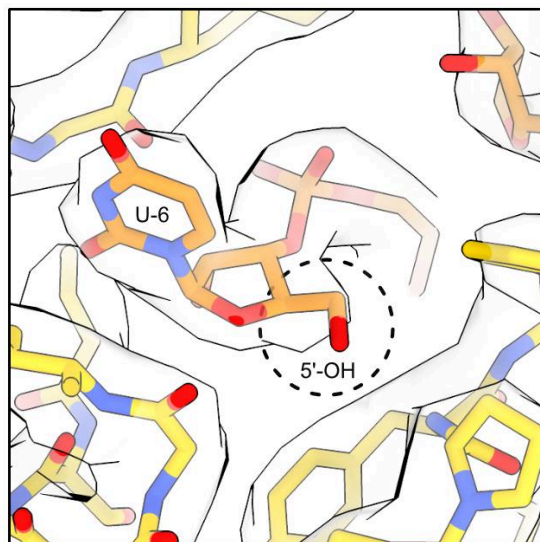
Supplementary Fig. 3 | Cryo-EM data processing for type IV-A3 in complex with DNA. **a** Processing workflow of the type IVA-3 DNA bound CRISPR complex. All steps performed in Cryosparc (v. 4.2). **b** FSC curve and angular distribution plot calculated in CryoSPARC (v. 4.2). The global resolution at FSC 0.143 is indicated by a solid blue line. **c** final reconstruction map colored according to local resolution.



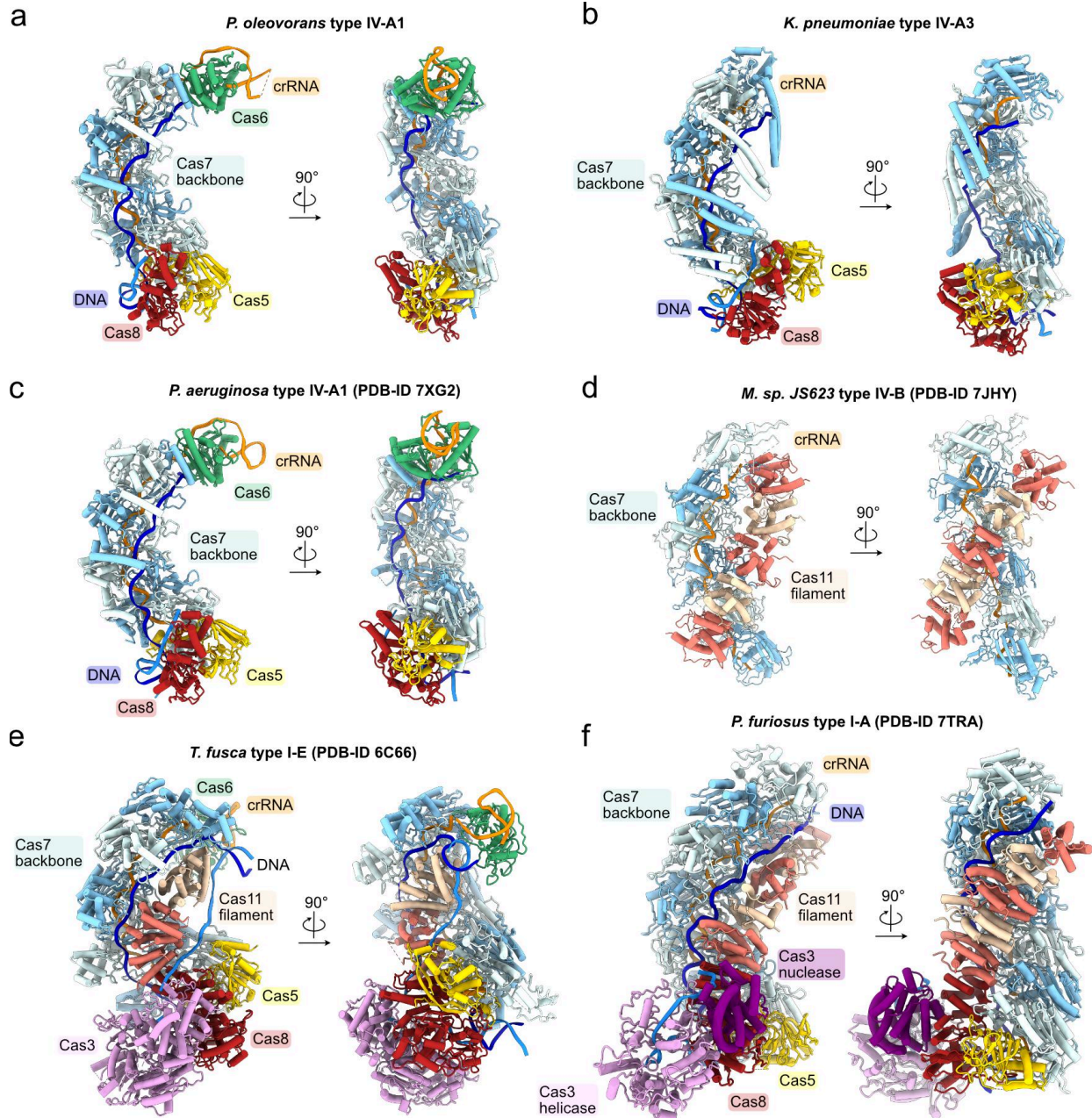
Supplementary Fig. 4 | Coordinates, experimental and EMReady-processed maps of type IV-A1 with and without DinG, and type IV-A3 in absence of DinG. Shown are model coordinates (cartoon) and maps (volumes) of type IV-A1 in absence (a) and presence of DinG (b), as well as type IV-A3 in absence of DinG (c). Experimental unfiltered and sharp maps, as well as EMReady processed maps are shown and labeled accordingly. The EMReady map in (b) is shown contoured at two different levels. Magenta volumes indicate unmodelled regions.



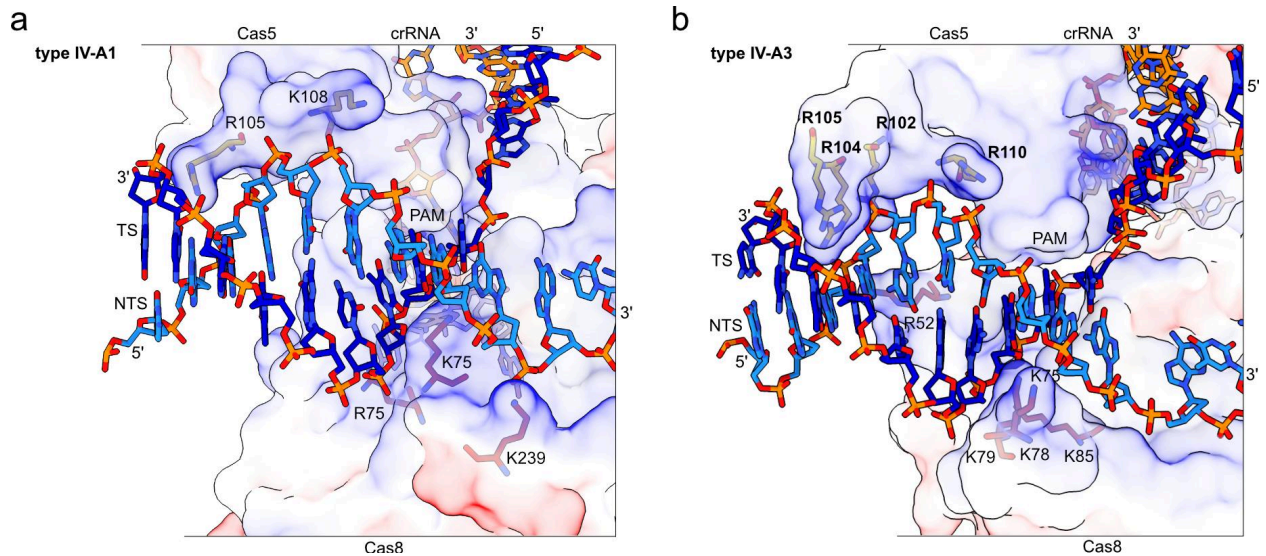
Supplementary Fig. 5 | The terminal Cas7 and Cas6 are poorly resolved in type IV-A3. a Structure model of the type IV-A3 effector bound to DNA in three 90°-rotated views. **b** and **c** Unfiltered (**b**) and EMReady (**c**) cryo-EM maps of the type IV-A3 effector in three 90°-rotated views, corresponding to the orientations shown in **a**. Magenta colored map segments highlight regions not covered by the model shown in **a**.

a**b**

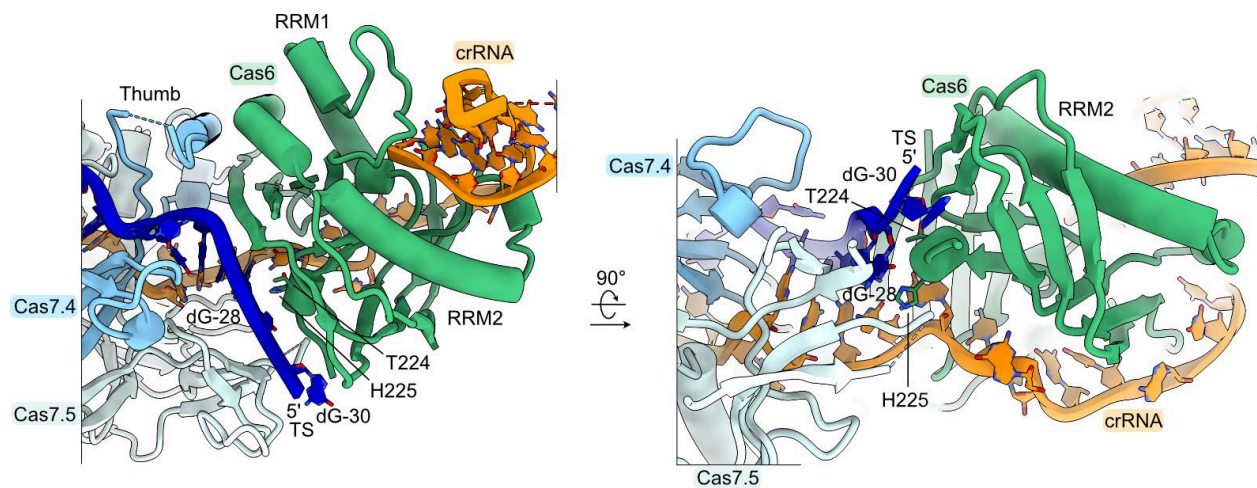
Supplementary Fig. 6 | crRNA 5'-end chemistry in type IV-A1 and type IV-A3. a Sharpened experimental cryo-EM map (white translucent surface) and model of the type IV-A1 effector showing the crRNA 5'-end (dashed circle). crRNA and Cas5 are shown as orange and yellow sticks, respectively. **b** Sharpened experimental cryo-EM map and model of the type IV-A3 effector showing the crRNA 5'-end (dashed circle). The crRNA and Cas5 are shown as orange and yellow sticks, respectively.



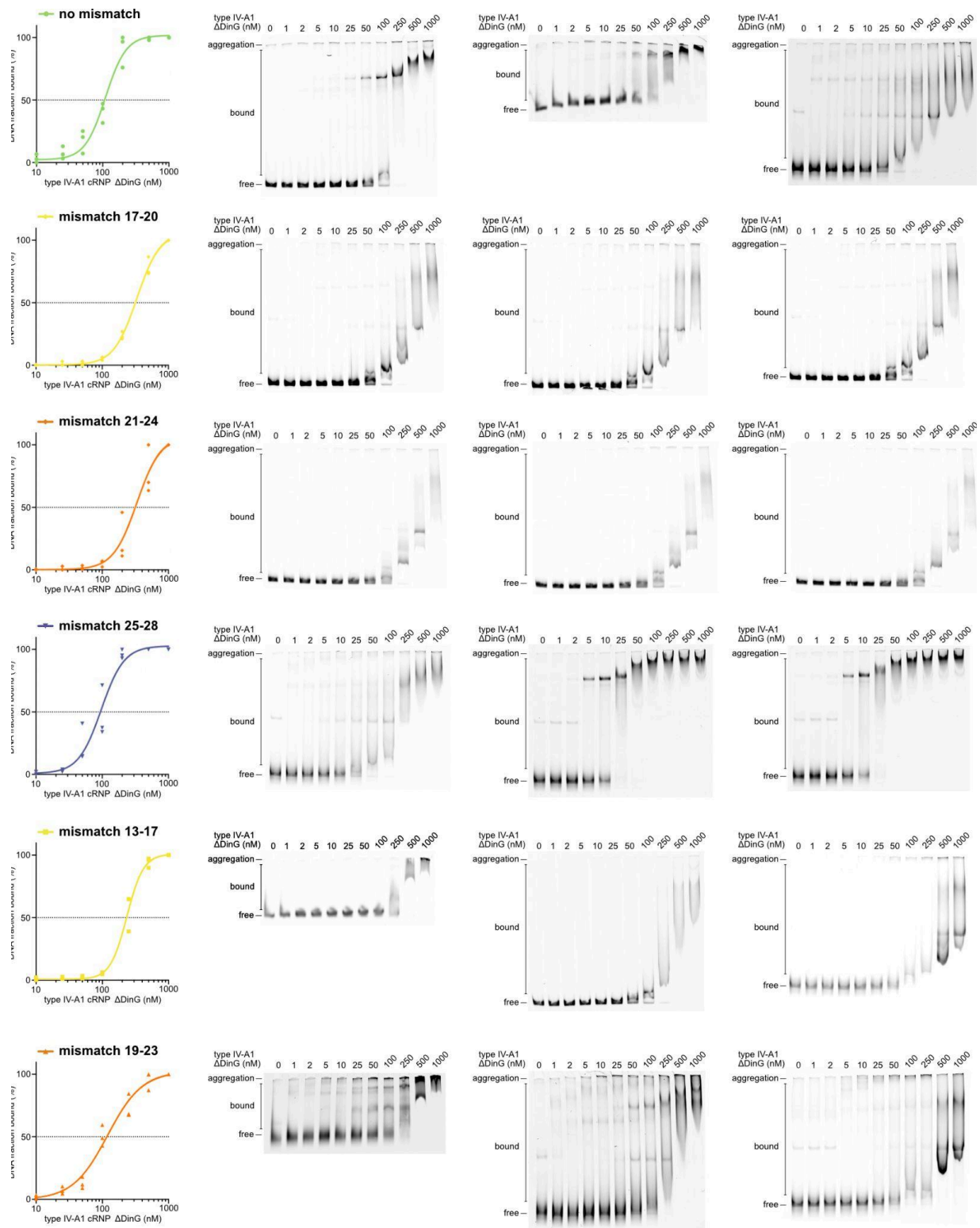
Supplementary Fig. 7 | Comparison of type IV and type I effector structures. **a** and **b** Type IV-A1 (**a**) and type IV-A3 (**b**) effector structures in complex with DNA (this study). **c** Cryo-EM structure of *P. aeruginosa* type IV-A1 in complex with DNA (PDB-ID 7XG2²). **d** Partial cryo-EM structure of *M. sp. JS623* type IV-B in the absence of a cognate target (PDB-ID 7JHY³). **e** Cryo-EM structure of *T. fusca* type I-E in presence of DNA and Cas3 in the pre-nicking state (PDB-ID 6H66⁴). **f** Cryo-EM structure of *P. furiosus* type I-A effector-Cas3 in presence of DNA (PDB-ID 7TRA⁵).



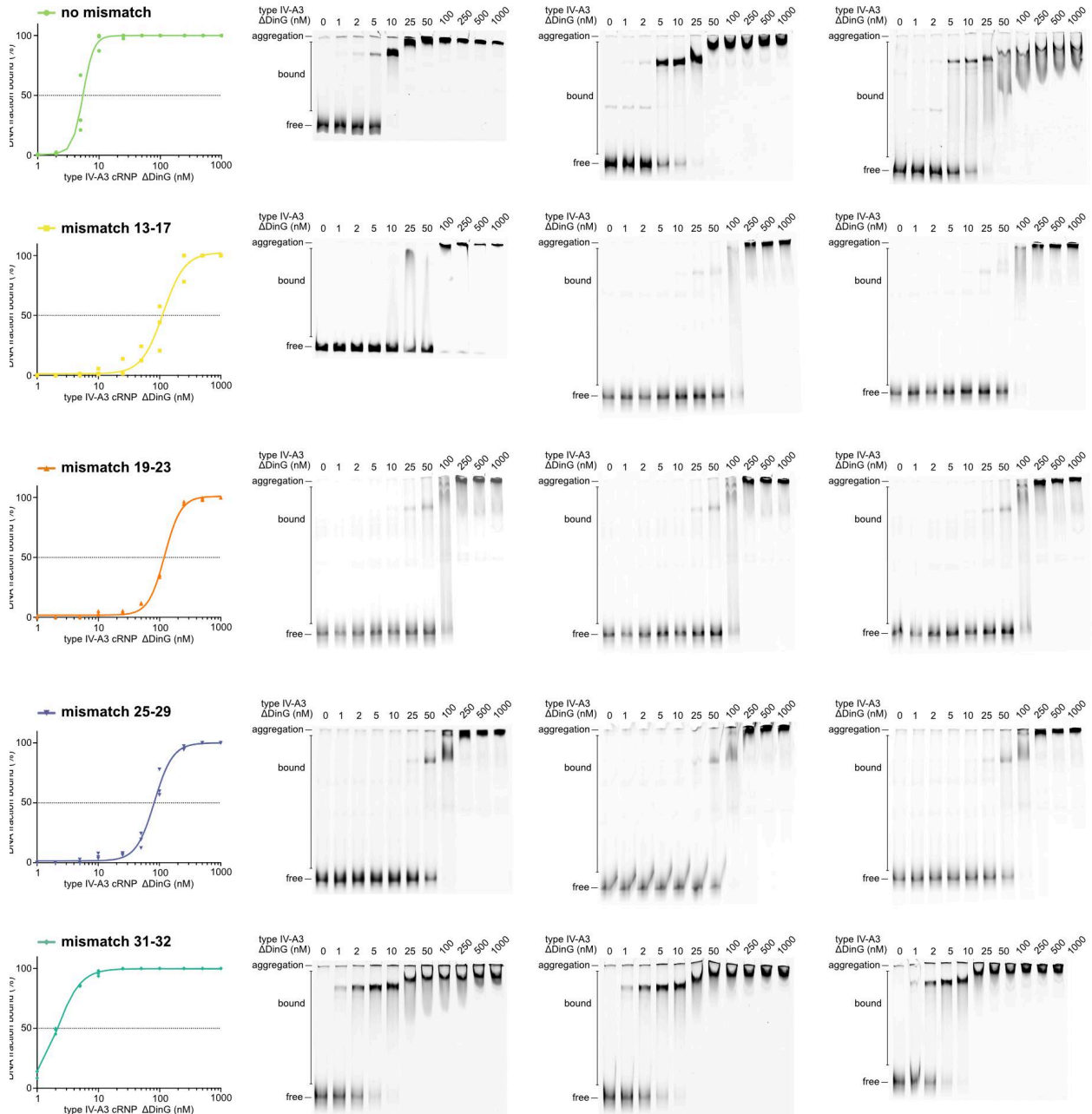
Supplementary Fig. 8 | Cas8 and Cas5 form a positively charged vice to recruit the PAM. **a** and **b** Shown is the PAM proximal dsDNA segment bound to the positively charged vice in the type IV-A1 effector (**a**) and the type IV-A3 effector (**b**). Blue surfaces indicate positive, and red surfaces indicate negative polarization. Arginine and lysine residues of Cas5 (yellow) and Cas8 (red) contacting the dsDNA segment are shown as yellow and red sticks, respectively. Amino acids producing interference defects upon substitution are highlighted in bold (data is shown in Fig. 2e).



Supplementary Fig. 9 | Type IV-A1 Cas6 caps the crRNA:TS hybrid. Shown is a Cas6-centered view on the head of the type IV-A1 effector bound to DNA in two 90°-rotated orientations. Cas6 side chains in proximity to the terminal crRNA:TS base pair in position 28 are shown as sticks and labeled according to their identity.

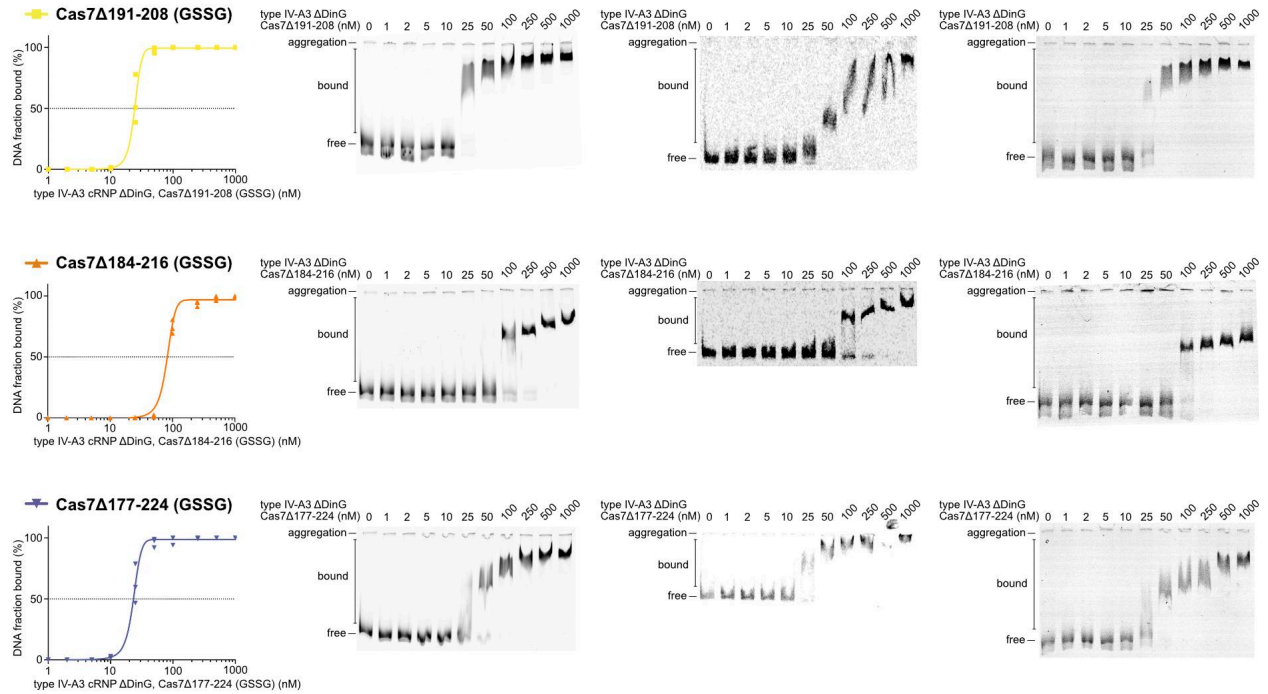


Supplementary Fig. 10 | EMSA assay probing the ability of type IV-A1 to bind mismatched DNA. Left: Graph showing the DNA binding efficiencies. Coloring corresponds to main text Figure 4E. Right: EMSA gels.

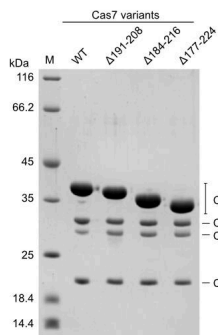


Supplementary Fig. 11 | EMSA assay probing the ability of type IV-A3 to bind mismatched DNA. Left: Graph showing the DNA binding efficiencies. Coloring corresponds to main text Figure 4F. Right: EMSA gels.

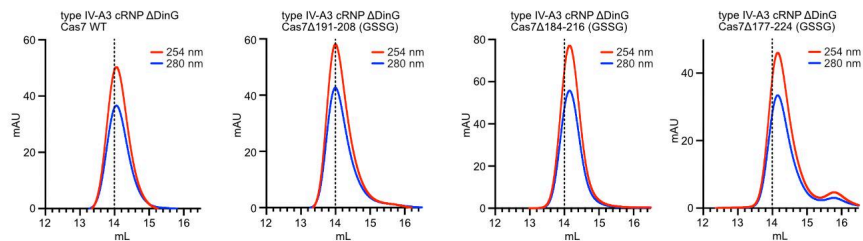
a



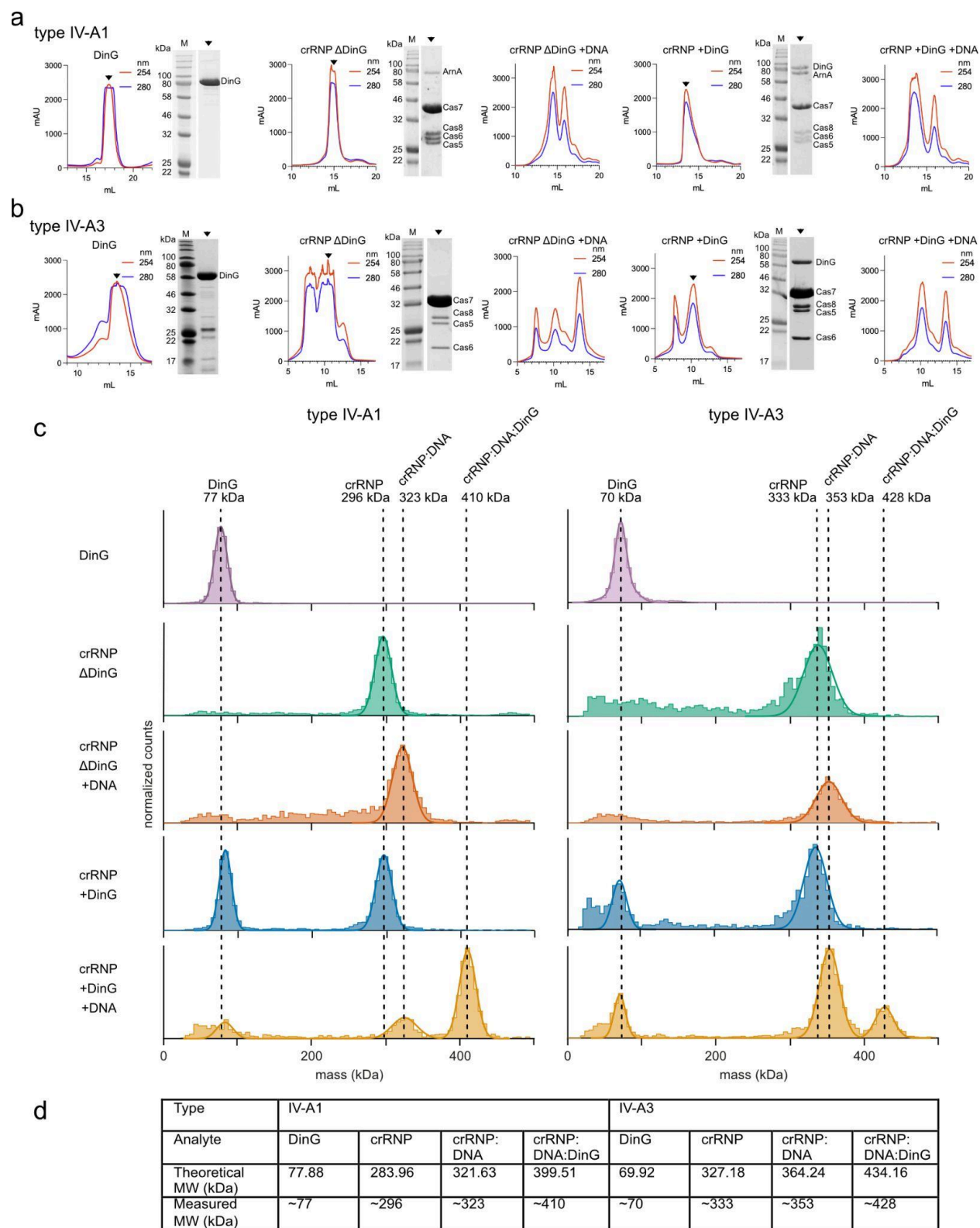
b



c

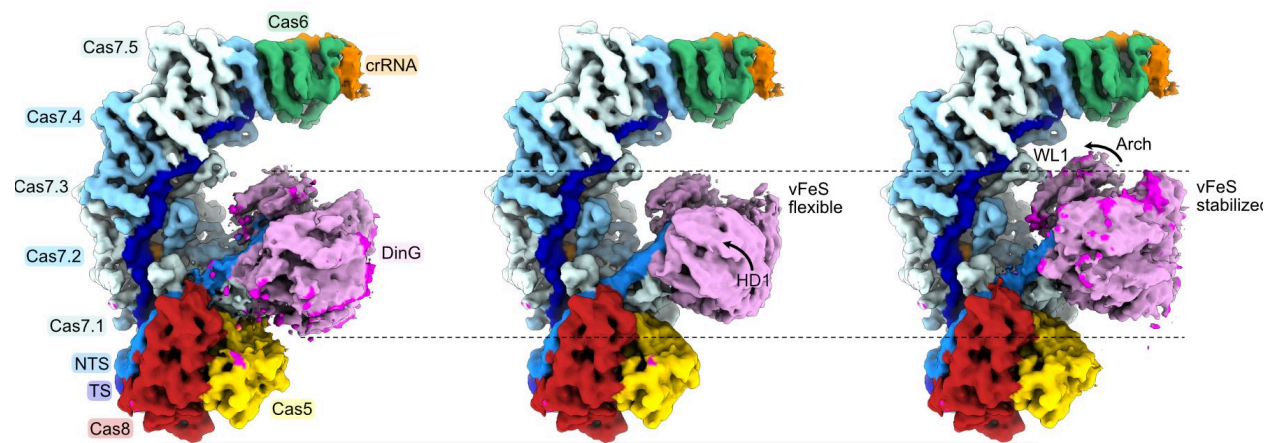


Supplementary Fig. 12 | EMSA assay probing the ability of type IV-A3 complexes containing Cas7 variants to bind DNA. a Left: Graph showing the DNA binding efficiencies. Coloring corresponds to main text Fig. 5d. Right: EMSA gels. **b** SDS-PAGE assessing the homogeneity of purified complexes. **c** Analytical size exclusion chromatography of type IV-A3 complexes containing Cas7 variants.

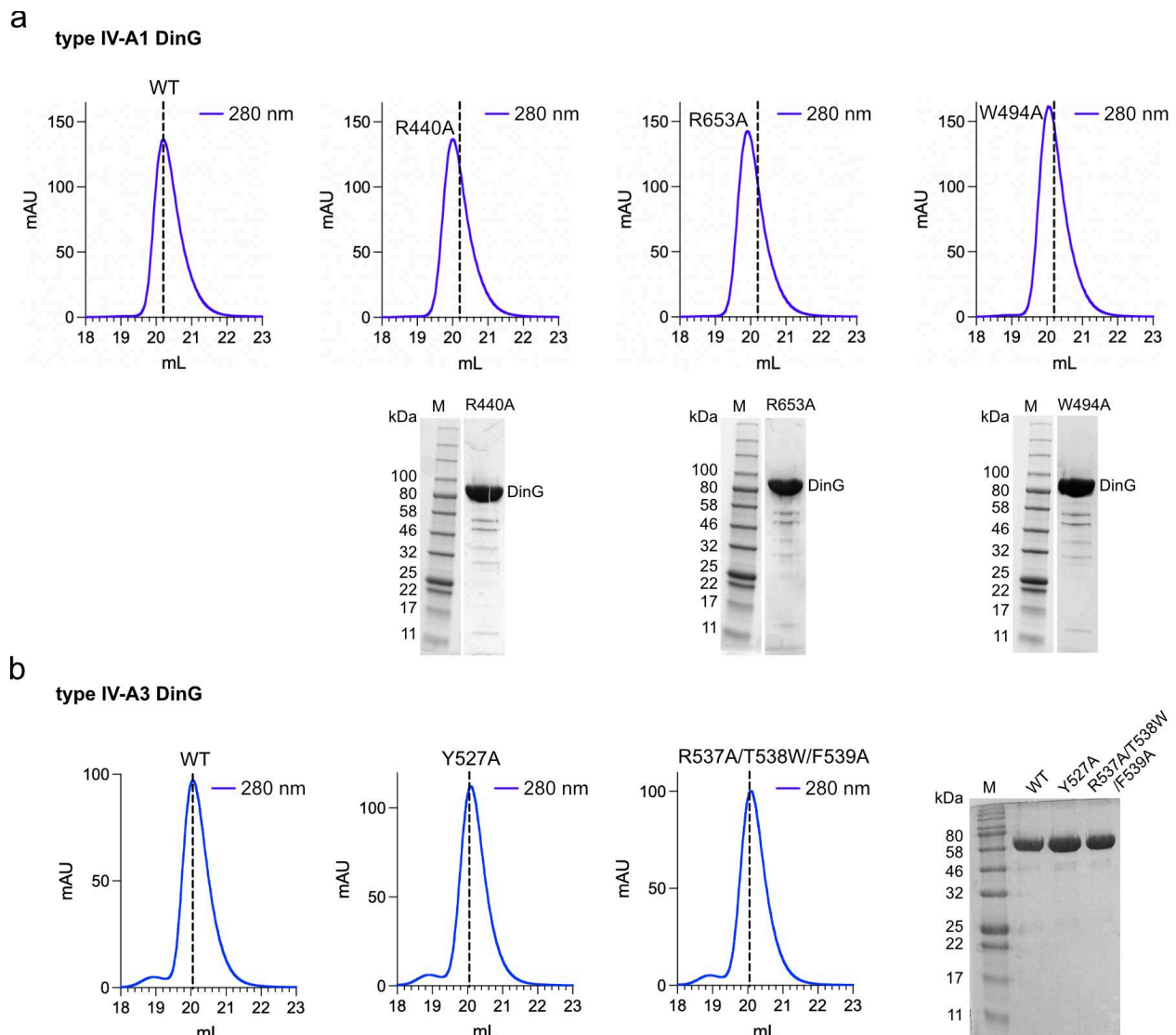


Supplementary Fig. 13 | Mass photometry of purified and reconstituted type VI-A complexes. **a** and **b** Preparative SEC traces of DinG and type IV CRISPR nucleoprotein (crRNP) complexes in the absence and presence of DinG and DNA of types IV-A1 (**a**) and IV-A3 (**b**), run on S6 10/300 and S200 10/300

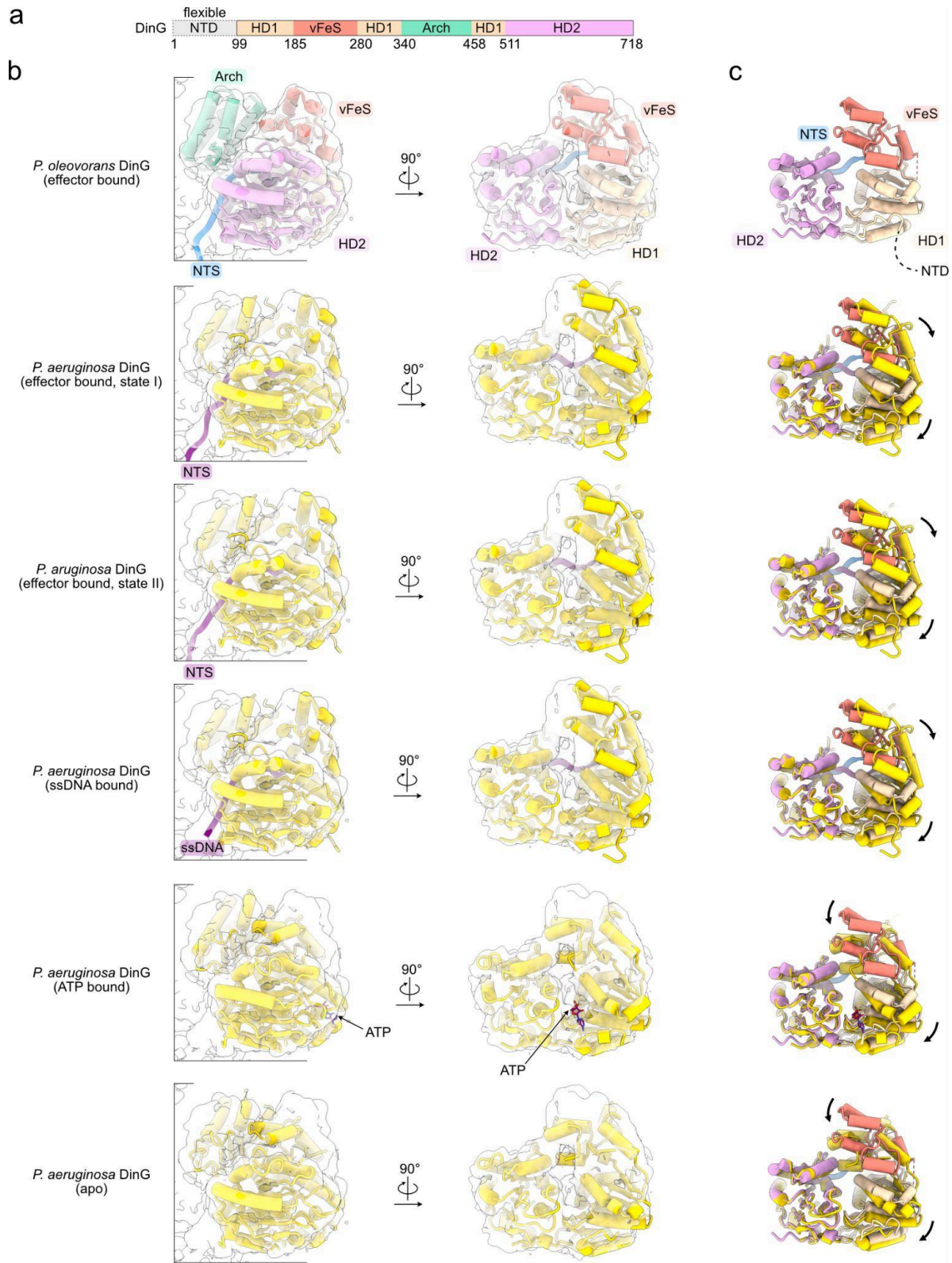
columns, respectively. Triangles indicate fractions analyzed via SDS-PAGE. **c** Mass photometric analysis of peak fraction from **a** and **b**. Dashed lines highlight the measured molecular weight of representative data. Measurements were repeated three times with similar results. **d** Table listing the theoretical and measured molecular weights of the analytes.



Supplementary Fig. 15 | 3D variability analysis (3DVA) of type IV-A1 effector bound to DNA and DinG. Shown are three representative frames of the 3DVA. Left: frame 1; center: frame 5; right: frame 10. Lines are shown to highlight the relative rearrangements in DinG. Arrows indicate domain rearrangements. Magenta colored map regions indicate densities not accounted for by our model.

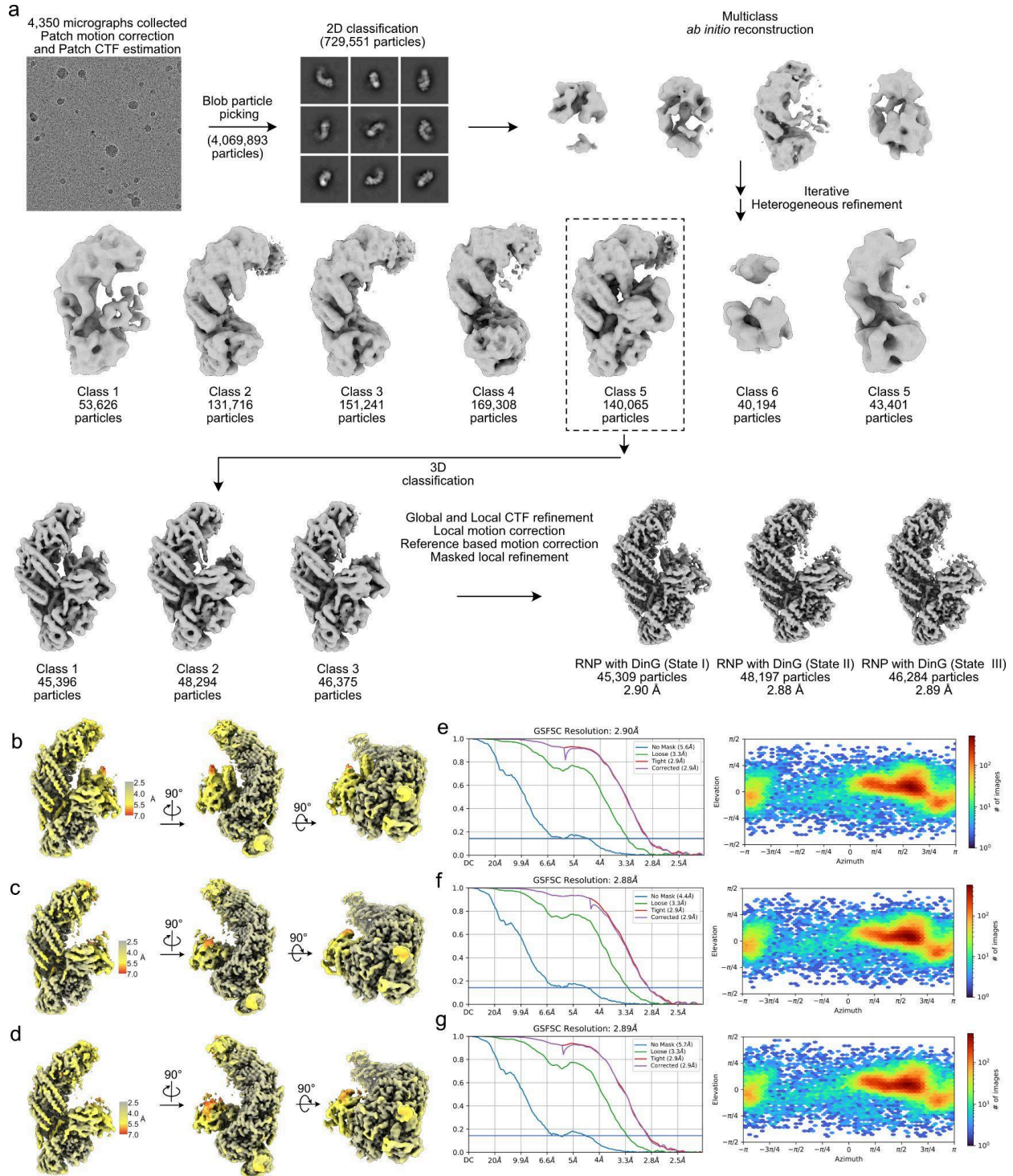


Supplementary Fig. 16 | Variant DinG proteins elute as single peaks during analytical size-exclusion chromatography. **a** Above: SEC traces of type IV-A1 variant DinG in comparison to WT DinG (left), recorded at 280 nm. Below: SDS-PAGES of preparative SEC fractions, used for analytical SEC runs. An SDS-PAGE for WT is shown in supplementary fig. 10A. **b** Center: SEC traces of type IV-A3 variant DinG in comparison to WT DinG (left). Right: SDS-PAGES of preparative SEC fractions, used for analytical SEC runs.

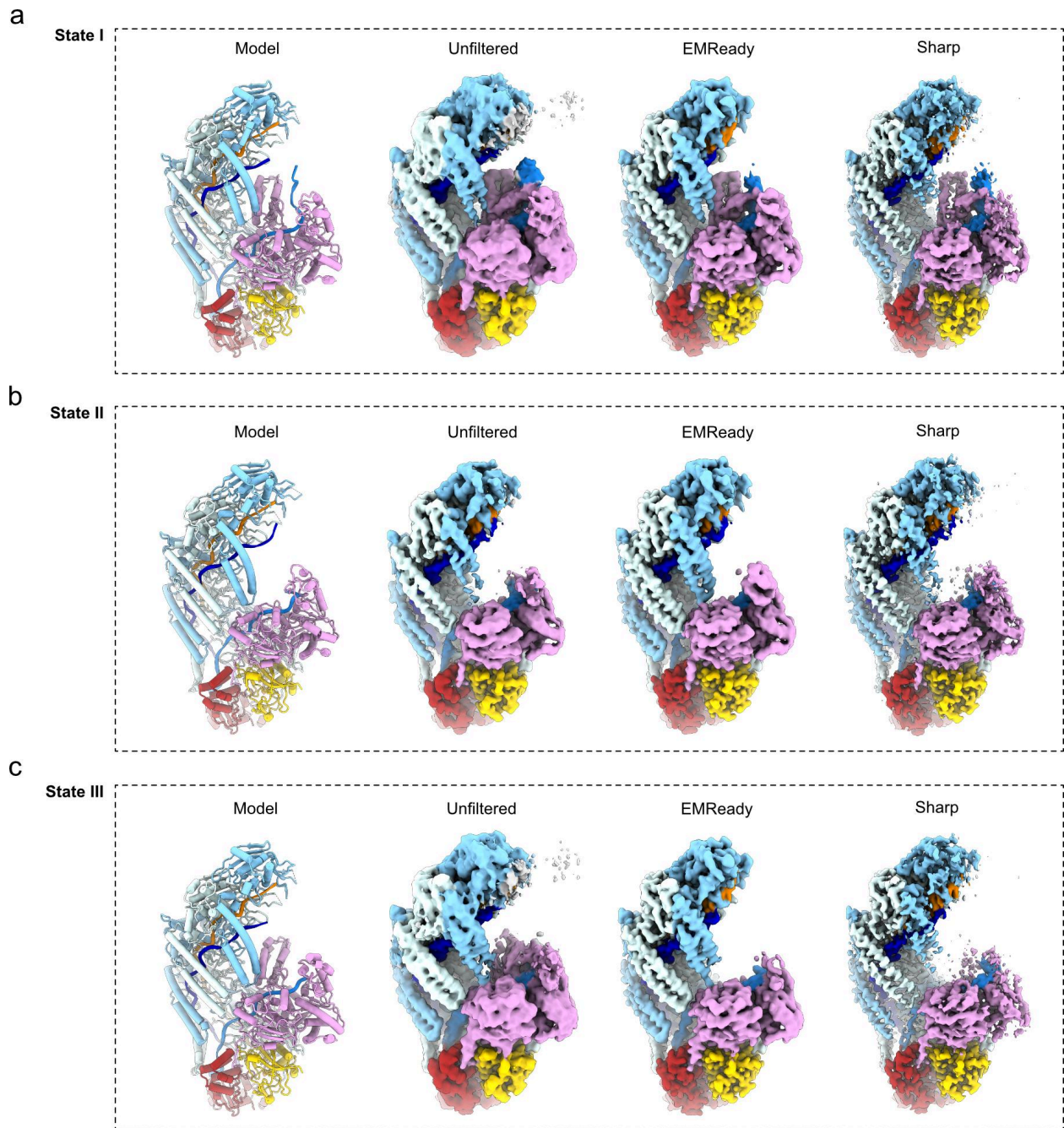


Supplementary Fig. 17 | Comparison of type IV-A1 DinG states. a Domain organization scheme of DinG. **b** Sharpened experimental cryo-EM map of the *P. oleovorans* type IV-A1 effector bound to DinG (

translucent white surface) and DinG states observed in this study (top, domain coloring as in **a**); and in supplementary ref. 2: PDB-IDs: 7XEX-A (apo), 7XF0-A (ATP), 7XF1 (ssDNA), 7XG3 (effector, state I), 7XG4 (effector state II), with DinG colored in yellow and nucleic acids in purple. Structures were superimposed according to the HD2 domain to highlight relative rearrangements. Arrows indicate domain rearrangements observed between the superimposed states.

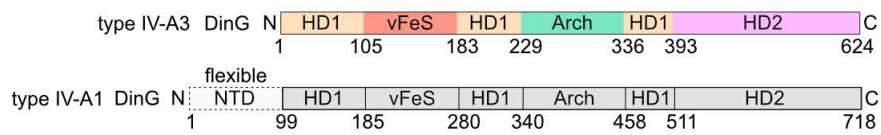


Supplementary Fig. 18 | Cryo-EM data processing for type IV-A3 in complex with DinG. a Processing workflow of the DNA-bound type IV-A3 effector complex in presence of DinG. All steps performed in CryoSPARC (v. 4.4). **b-d** Local resolution map, calculated in CryoSPARC (v. 4.4) for the type IV-A3 complex in the presence of DinG state I (**b**), state II (**c**), state III (**d**). **e-g** FSC curves calculated in CryoSPARC (v. 4.4) and orientation distribution of the final set of refined particles for state I (**e**), state II (**f**), state III (**g**). The global resolution at 0.143 is indicated by a solid blue line.

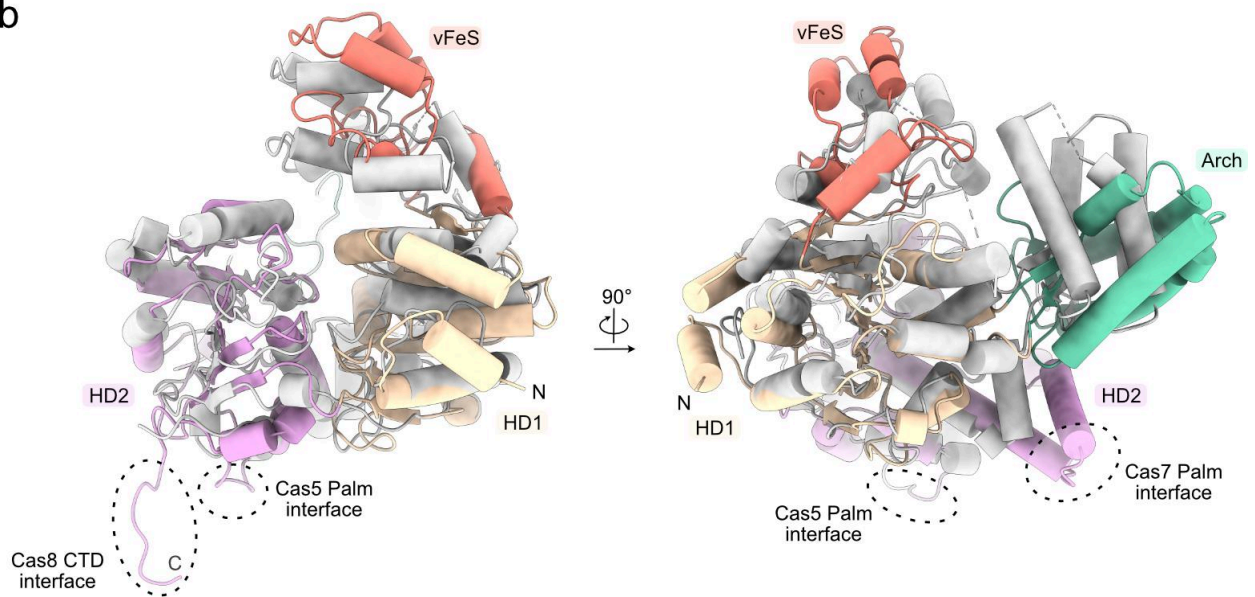


Supplementary Fig. 19 | Coordinates, experimental and EMReady-processed maps of type IV-A3 in presence of DinG. a, b and c Shown are model coordinates (cartoon) and maps (volumes) of type IV-A3 in presence of DinG for states I (**a**), II (**b**) and III (**c**). Experimental unfiltered and sharp maps, as well as machine learning processed maps (EMReady) are shown and labeled accordingly.

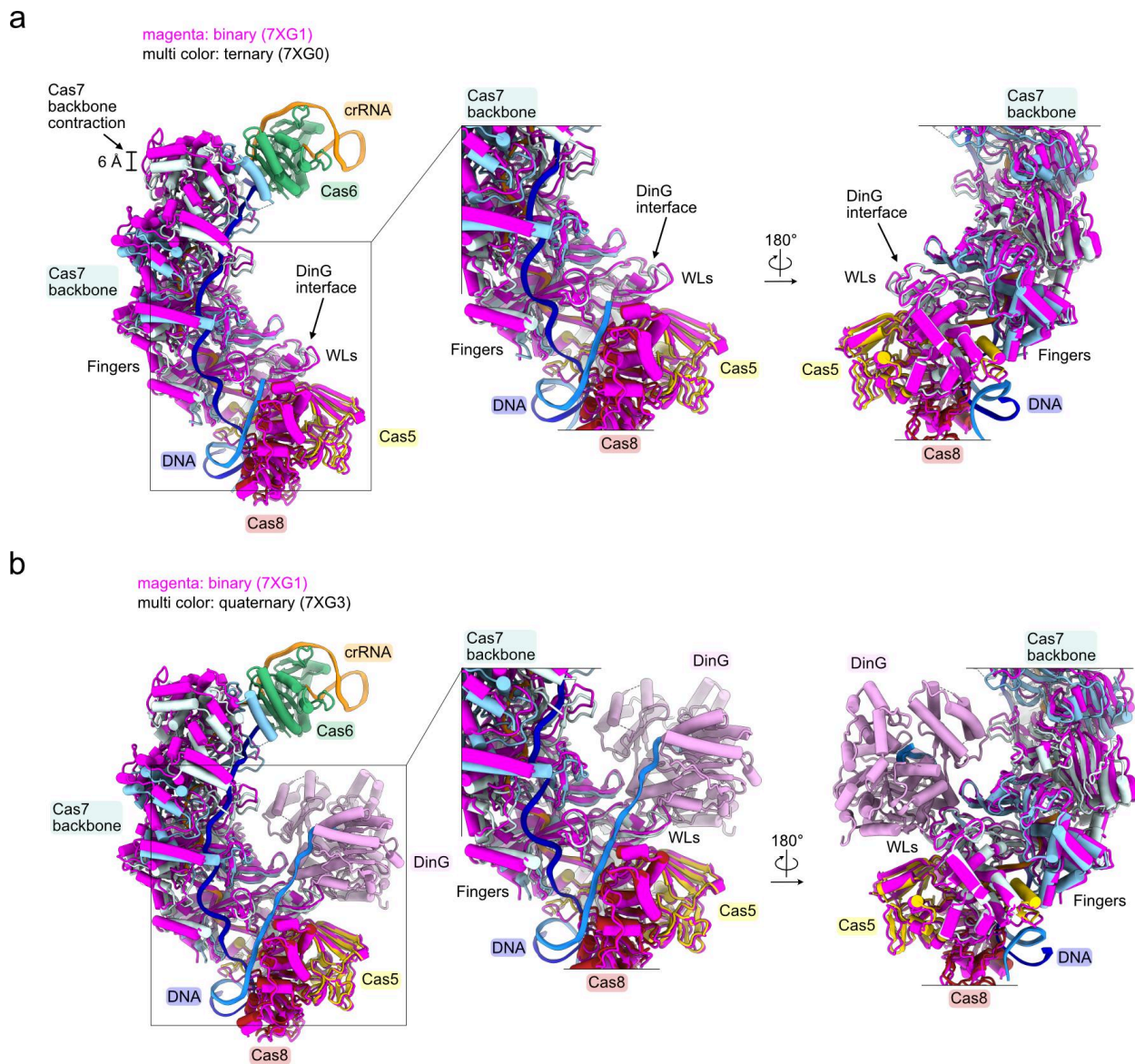
a



b



Supplementary Fig. 20 | Comparison of type IV-A1 and type IV-A3 DinG. **a** Domain organization scheme of DinG. **b** Superimposition of types IV-A1 and IV-A3 DinG (state I), as observed in complexes with DNA and the crRNP (not shown for clarity). Coloring as in **a**. crRNP interaction interfaces of type IV-A3 are indicated by dashed circles.



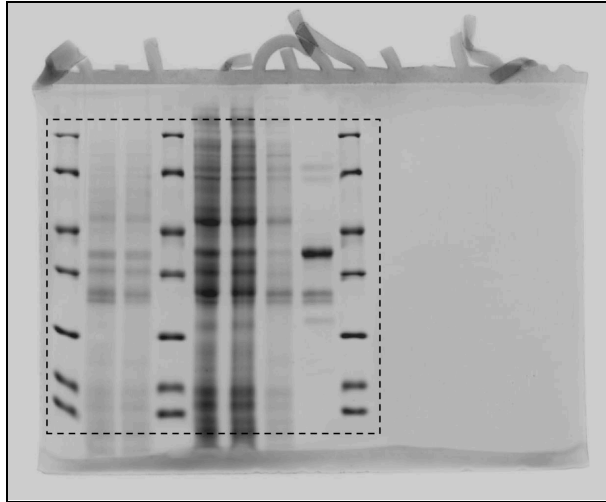
Supplementary Fig. 21 | Superimposition of *P. aeruginosa* type IV-A1 structures. **a** Left: superimposition of the binary (magenta, PDB-ID 7XG1²) and ternary states (colored according to subunits, PDB-ID 7XG0²). Structures were aligned based on Cas7.1. Right: Close-up view on the DinG interface in two 180°-rotated orientations. **b** Left: Superimposition of the binary (magenta, PDB-ID 7XG1²) and quaternary states (colored according to subunits, PDB-ID 7XG3²). Structures were aligned based on Cas7.1. Right: close-up view on the DinG interface in two 180°-rotated orientations.

SUPPLEMENTARY REFERENCES

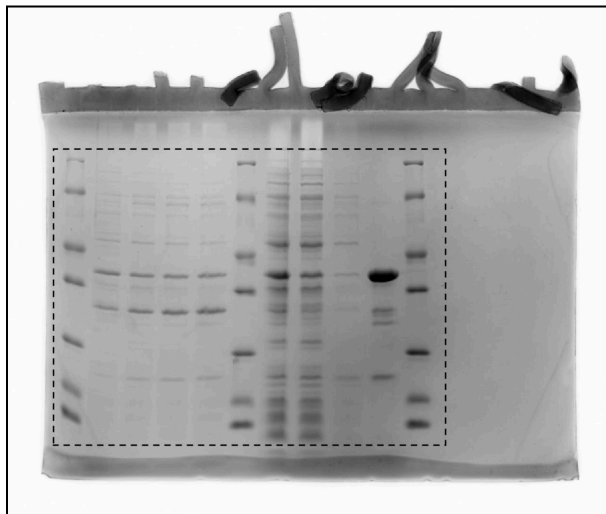
1. Benz, F. *et al.* Type IV-A3 CRISPR-Cas systems drive inter-plasmid conflicts by acquiring spacers in trans. *bioRxiv* 2023.06.23.546257 (2023) doi:10.1101/2023.06.23.546257.
2. Cui, N. *et al.* Type IV-A CRISPR-Csf complex: Assembly, dsDNA targeting, and CasDinG recruitment. *Mol. Cell* **83**, 2493–2508.e5 (2023).
3. Zhou, Y. *et al.* Structure of a type IV CRISPR-Cas ribonucleoprotein complex. *iScience* **24**, 102201 (2021).
4. Xiao, Y., Luo, M., Dolan, A. E., Liao, M. & Ke, A. Structure basis for RNA-guided DNA degradation by Cascade and Cas3. *Science* **361**, (2018).
5. Hu, C. *et al.* Allosteric control of type I-A CRISPR-Cas3 complexes and establishment as effective nucleic acid detection and human genome editing tools. *Mol. Cell* **82**, 2754–2768.e5 (2022).

SUPPLEMENTARY SOURCE DATA

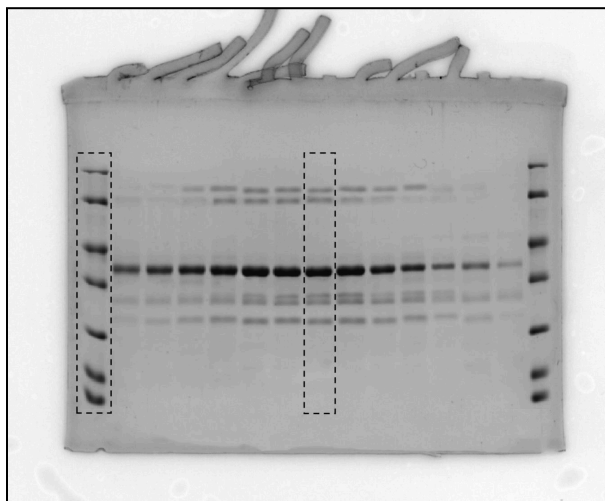
Supplementary Fig. 1b



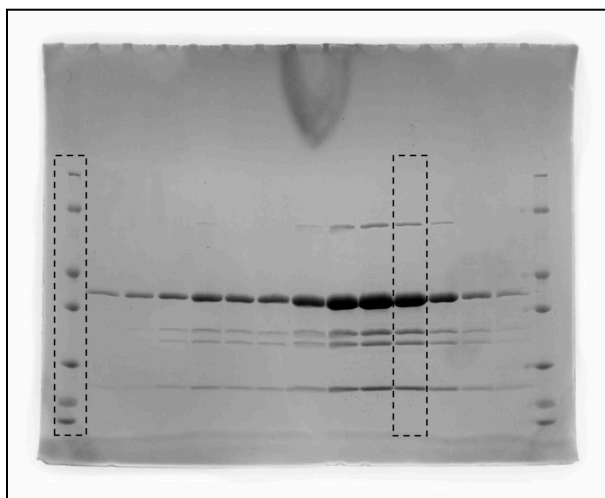
Supplementary Fig. 1c



Supplementary Fig. 1d

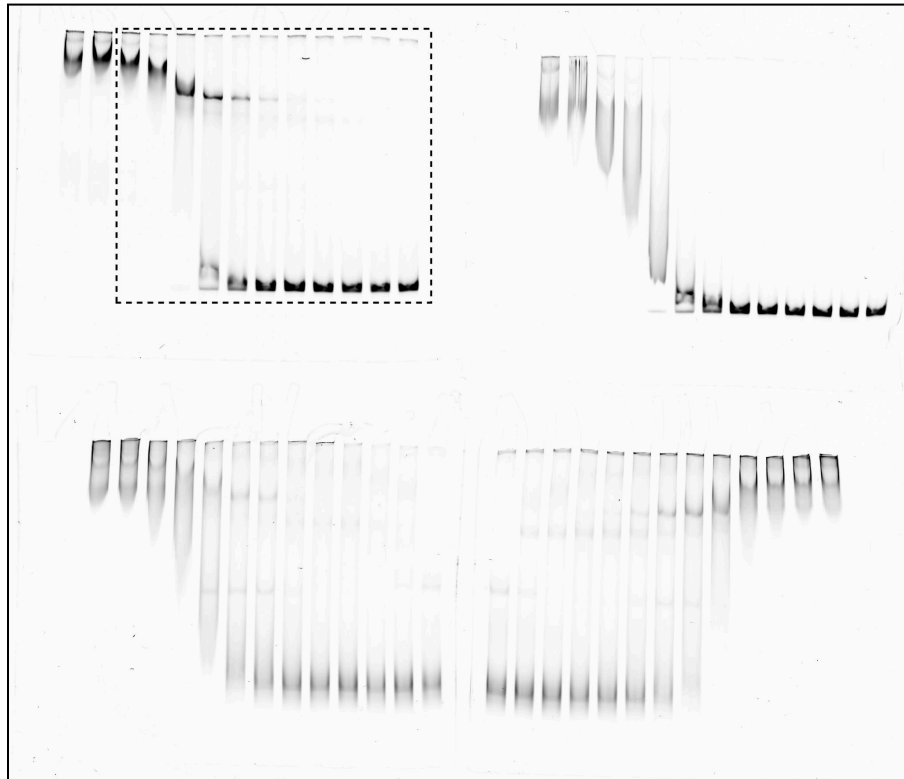


Supplementary Fig. 1e

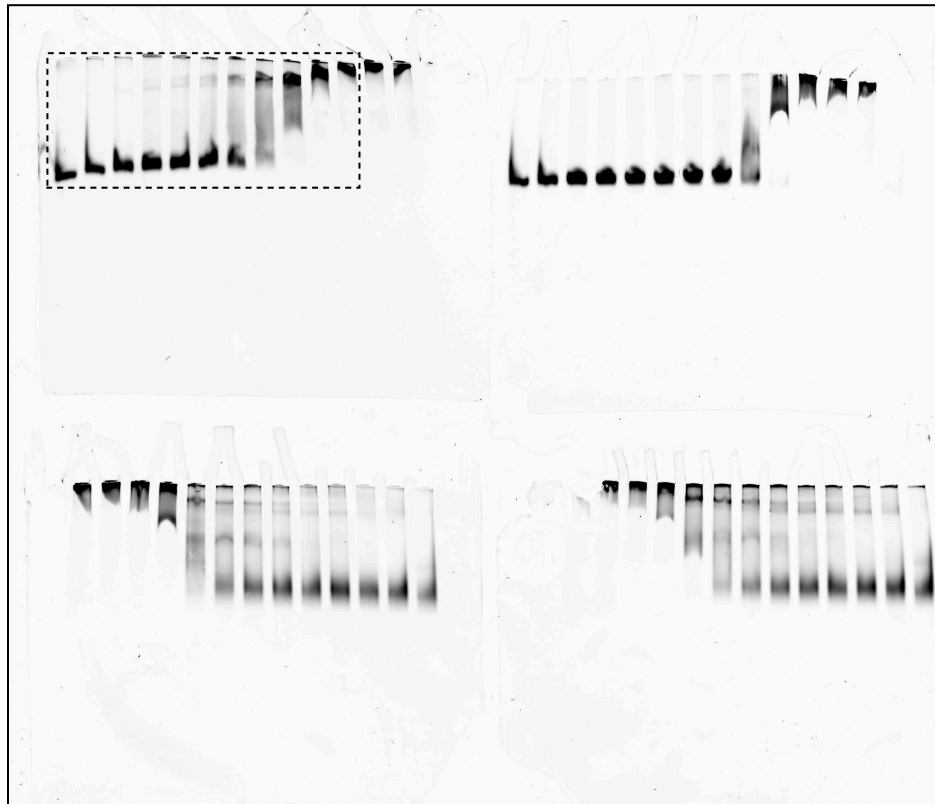


Supplementary Fig. 10

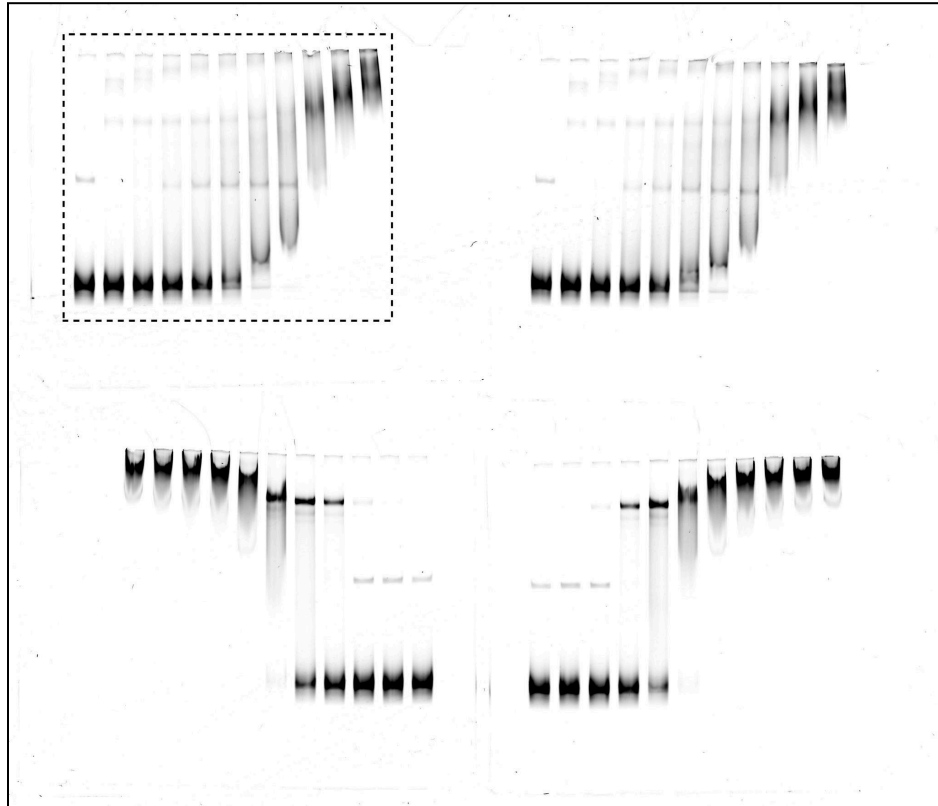
no mismatch: left panel



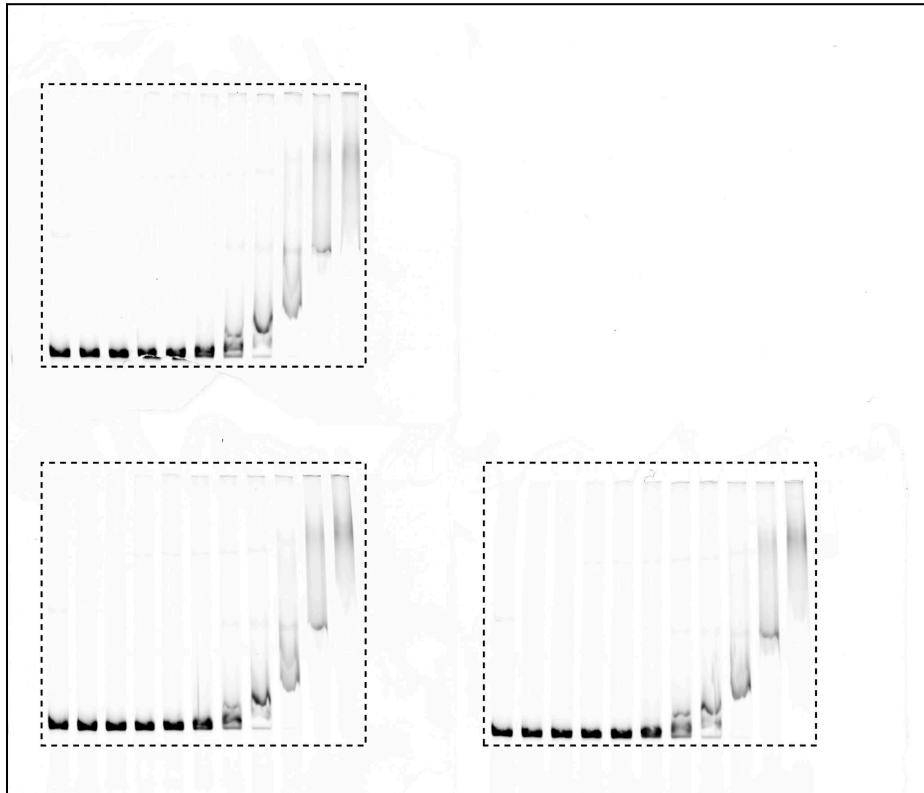
no mismatch; center panel



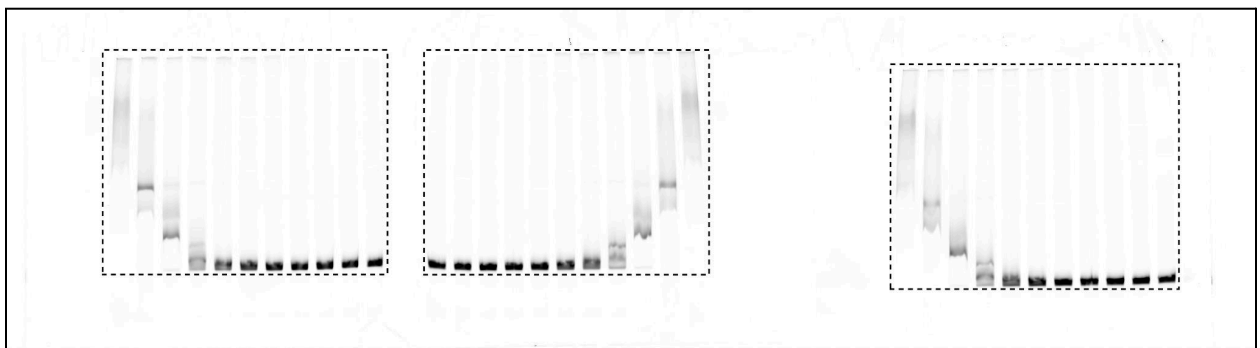
no mismatch; right panel



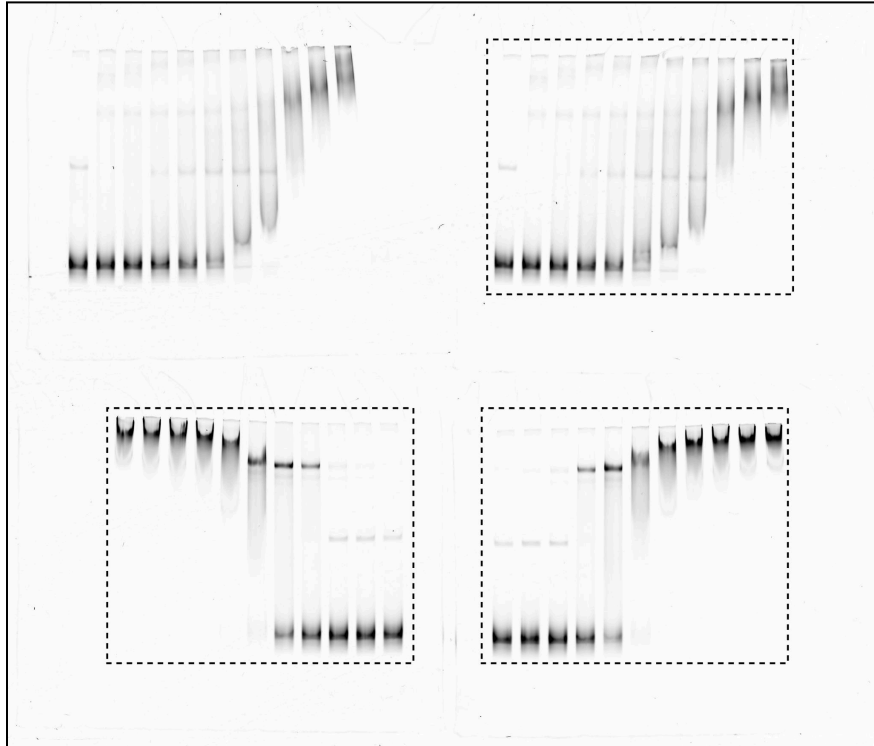
mismatch 17-20; left, center and right panel



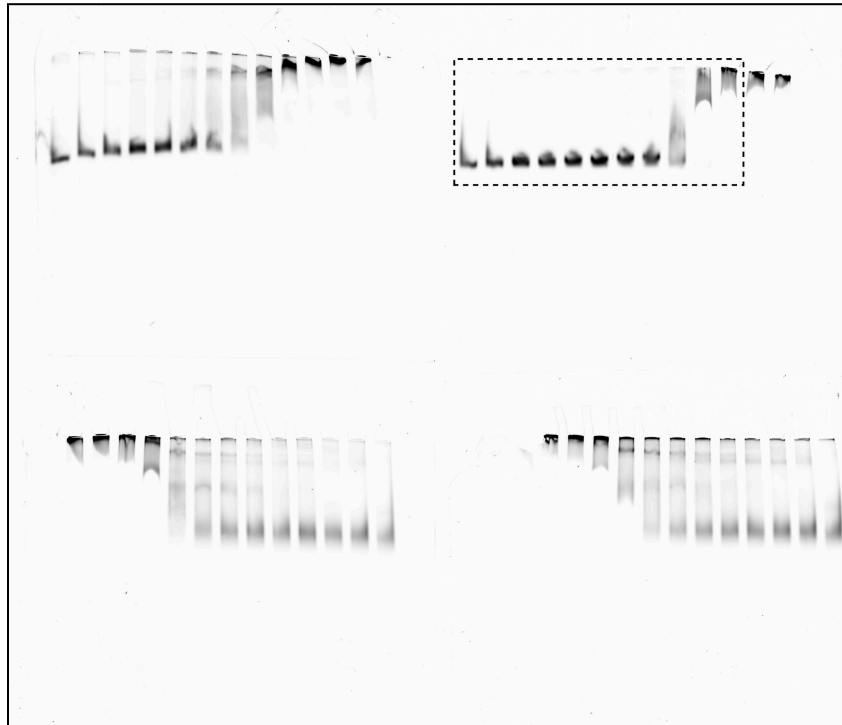
mismatch 21-24; left, center and right panel



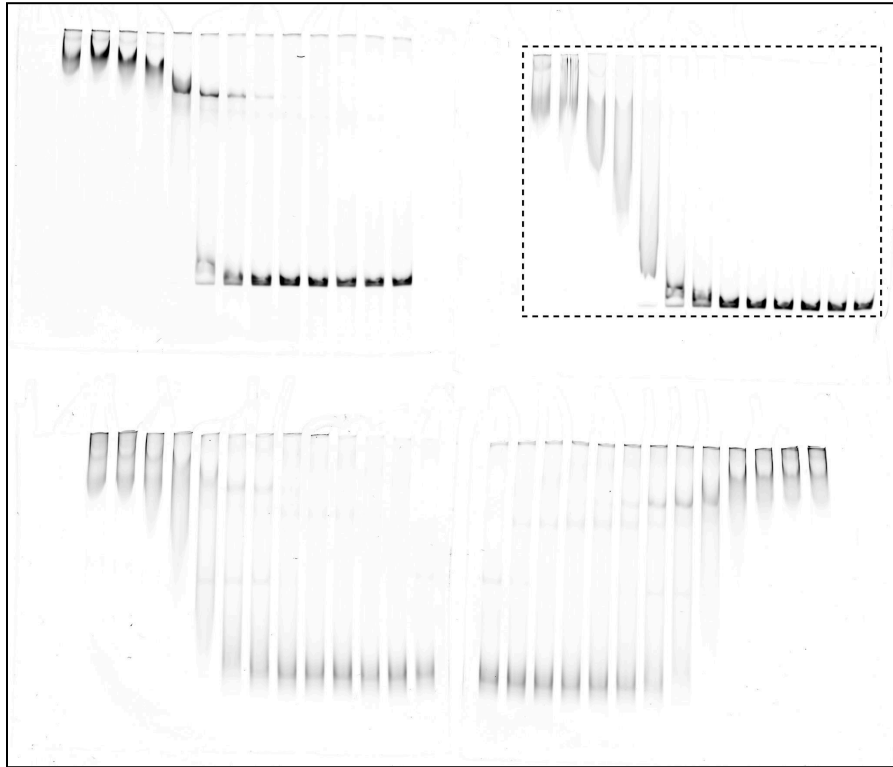
mismatch 25-28; left, center and right panel



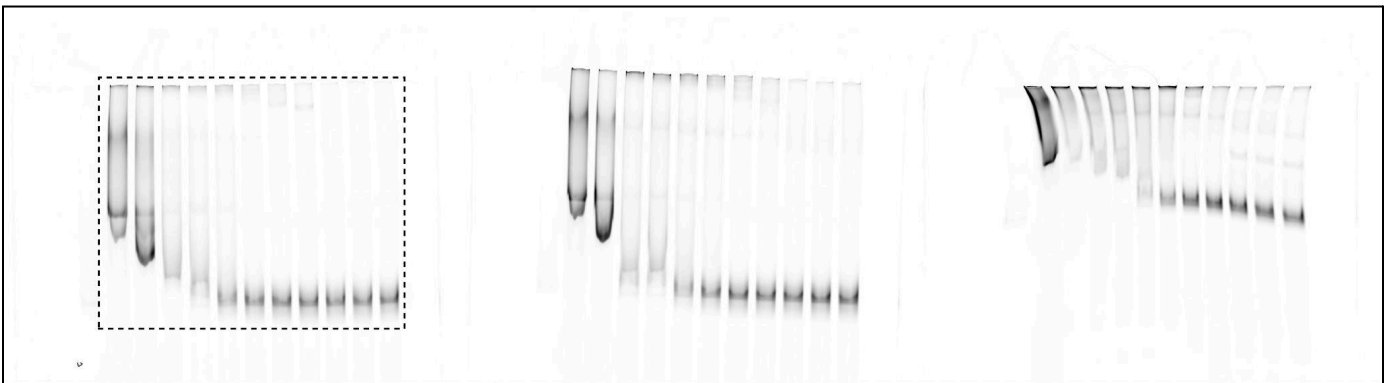
mismatch 13-17: left panel



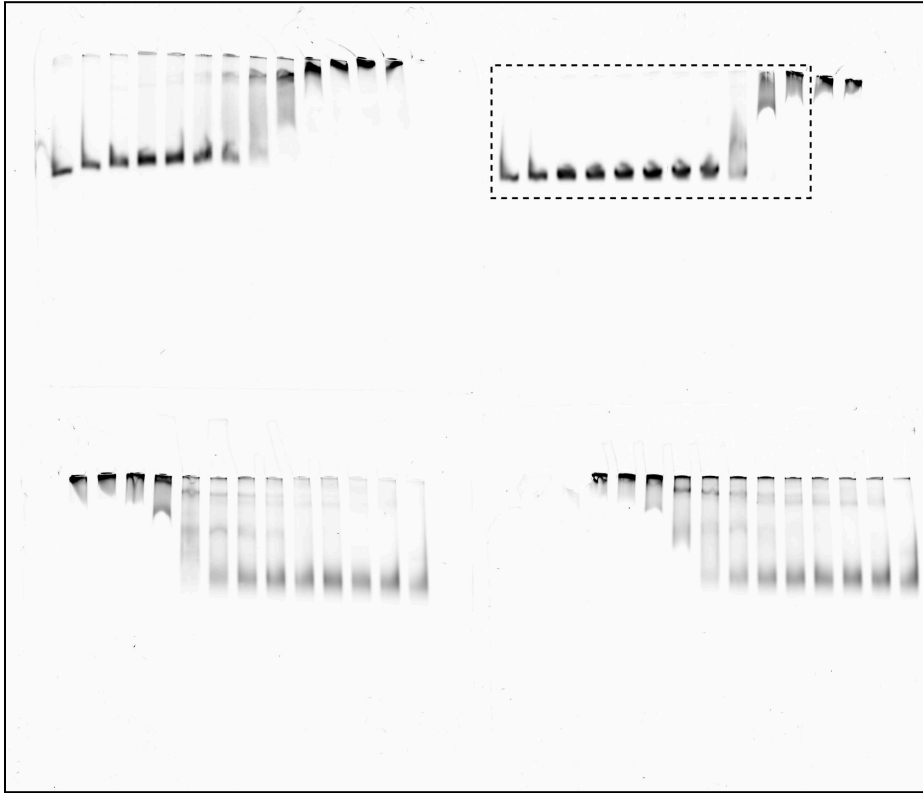
mismatch 13-17; center panel



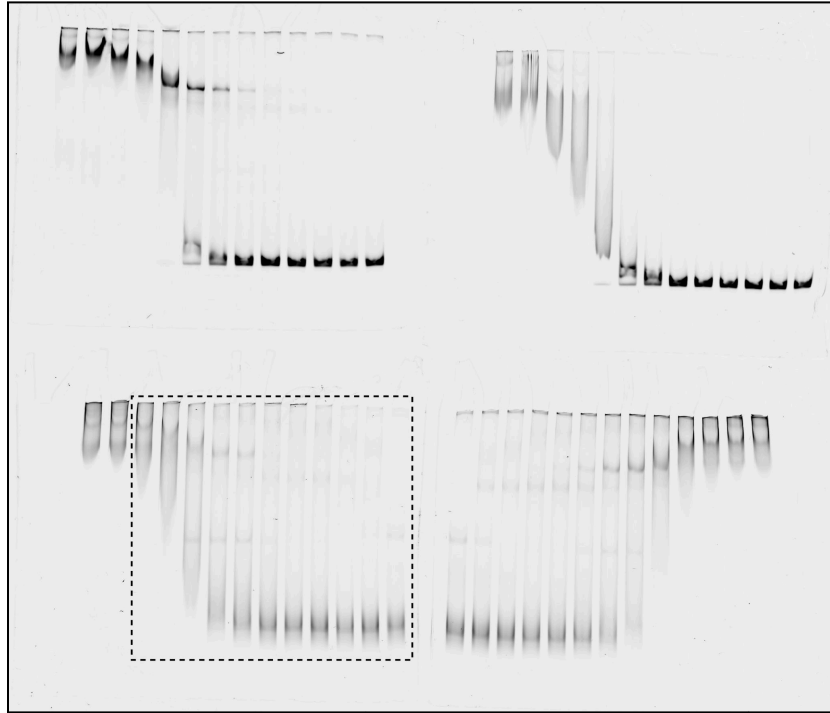
mismatch 13-17; right panel



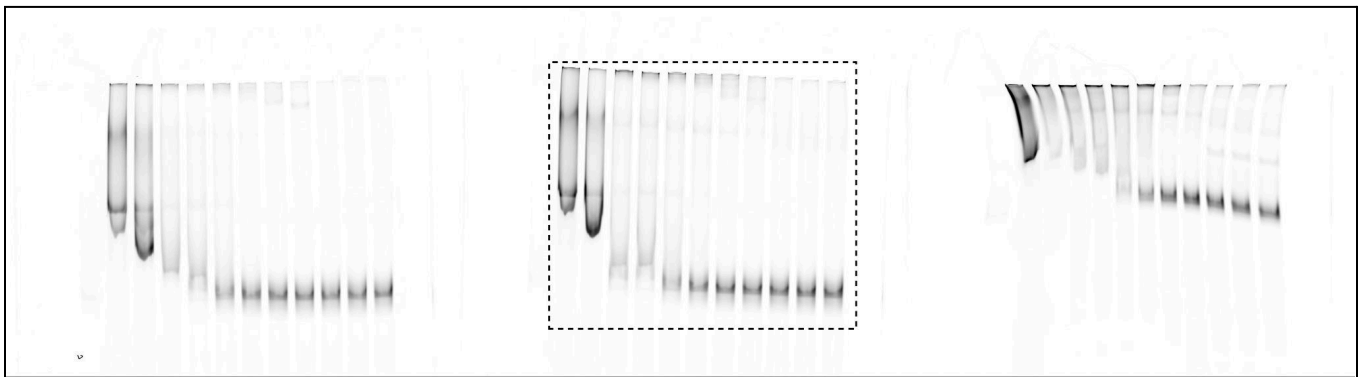
mismatch 19-23: left panel



mismatch 19-23; center panel

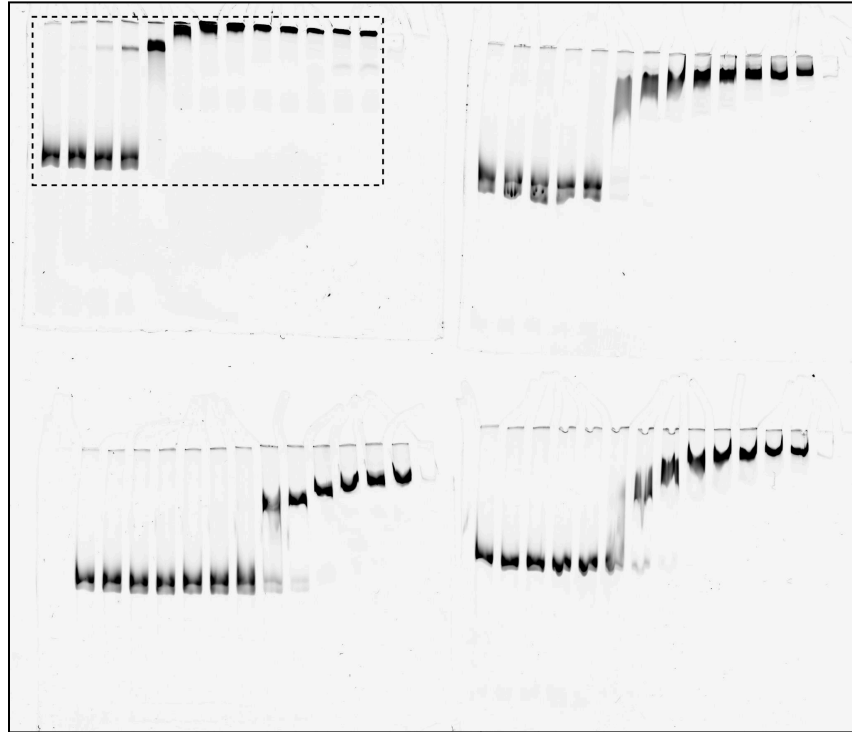


mismatch 19-23; right panel

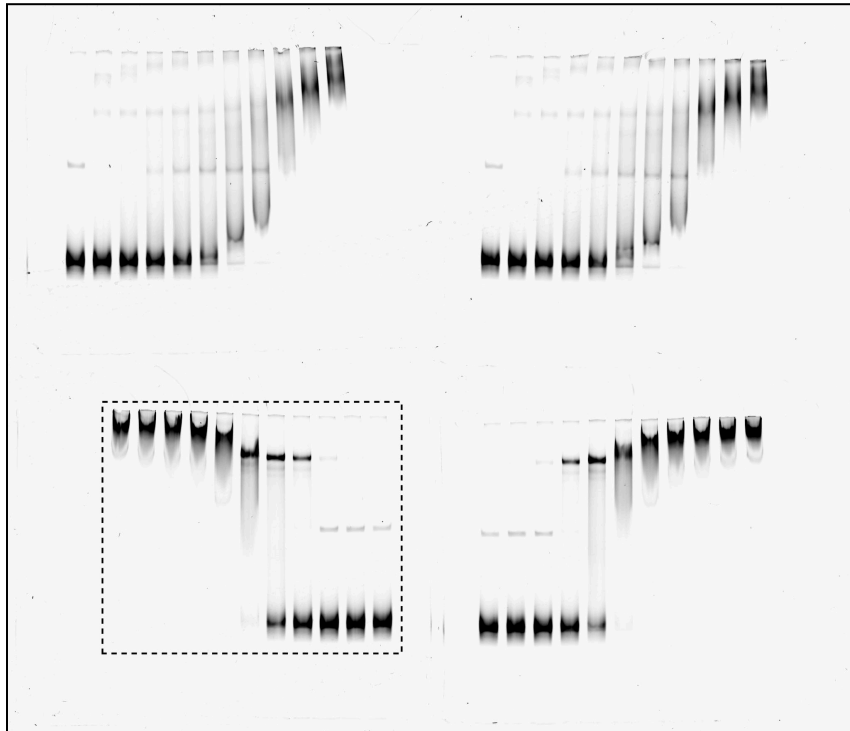


Supplementary Fig. 11

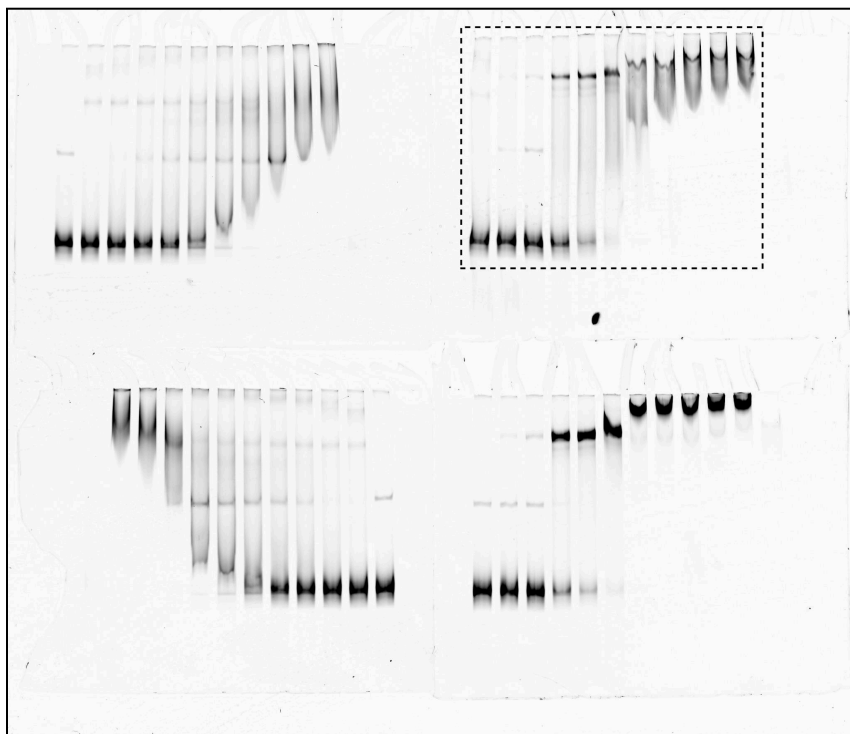
no mismatch; left panel



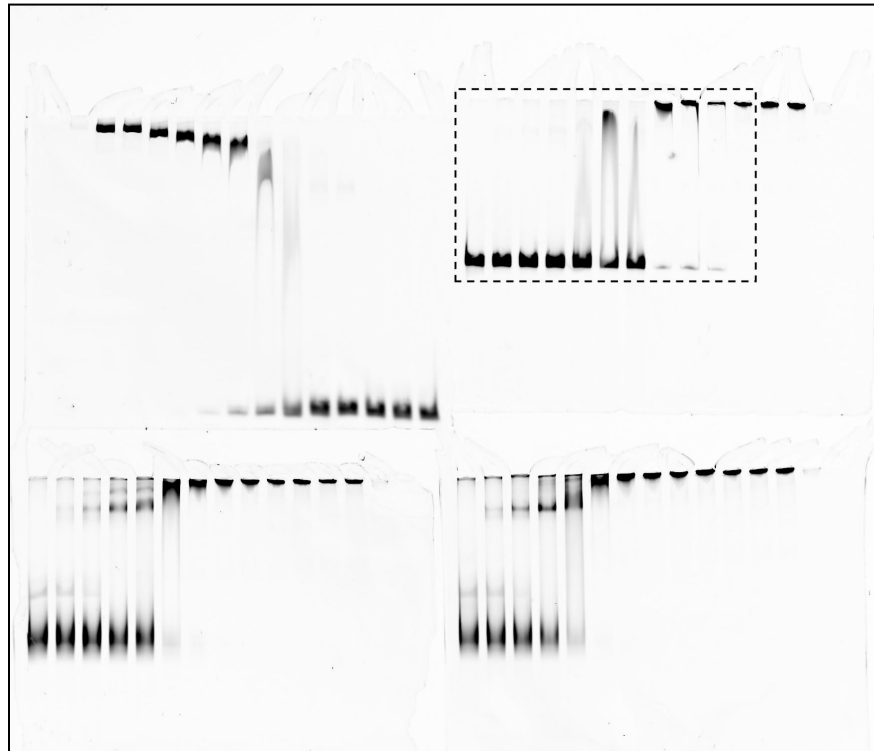
no mismatch; center panel



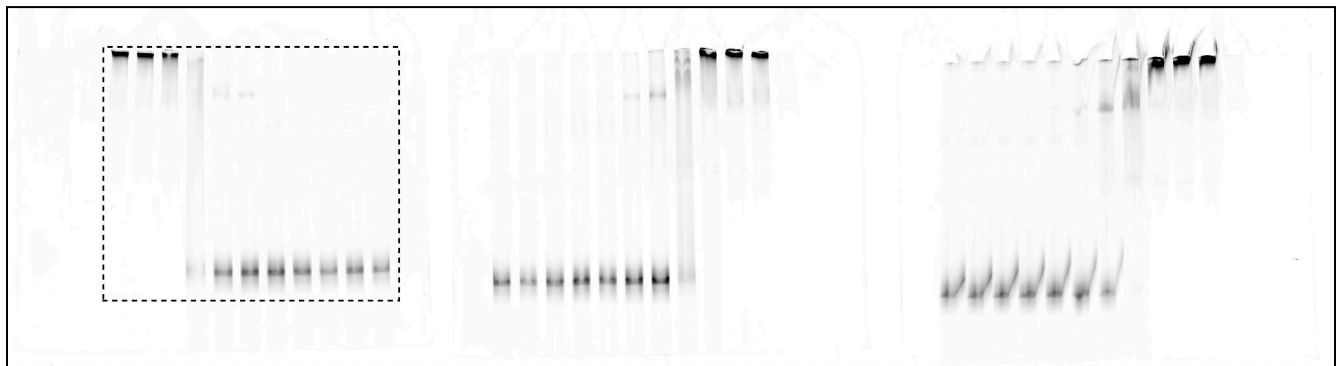
no mismatch; right panel



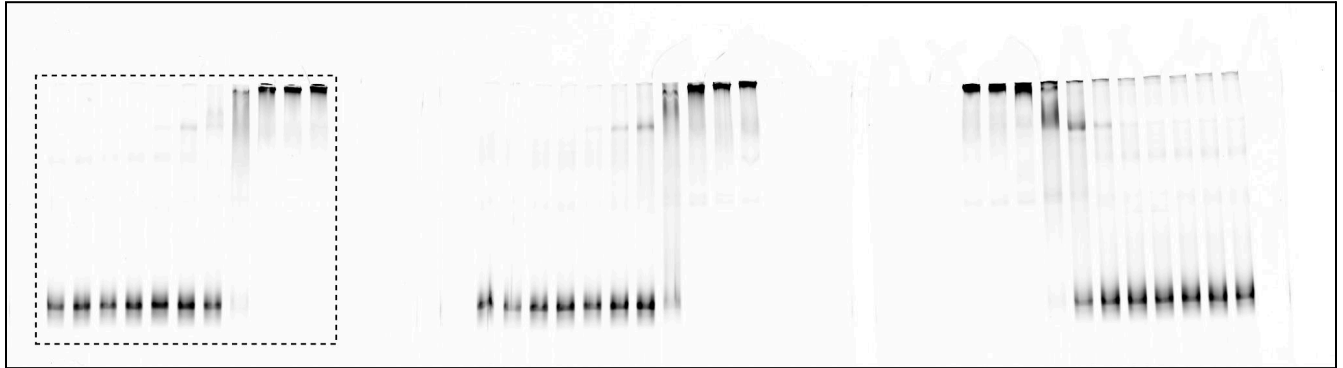
mismatch 13-17; left panel



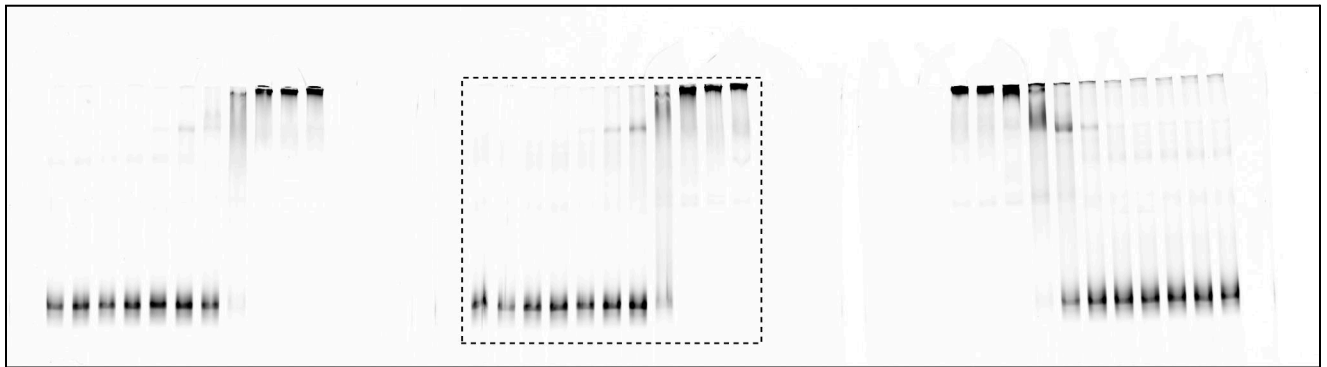
mismatch 13-17; center panel



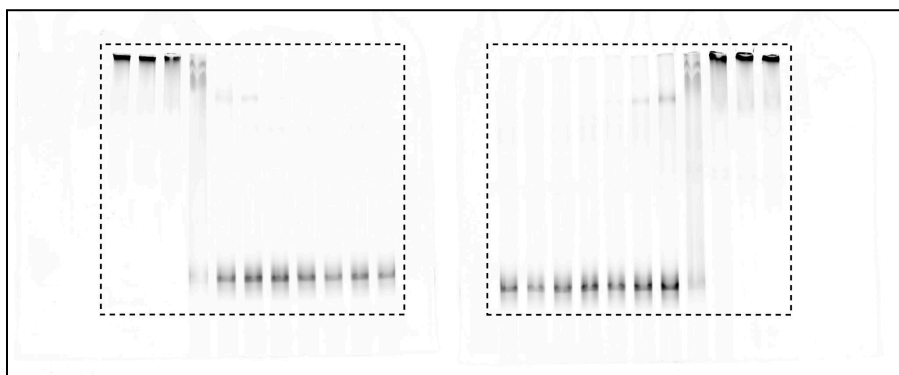
mismatch 13-17; right panel



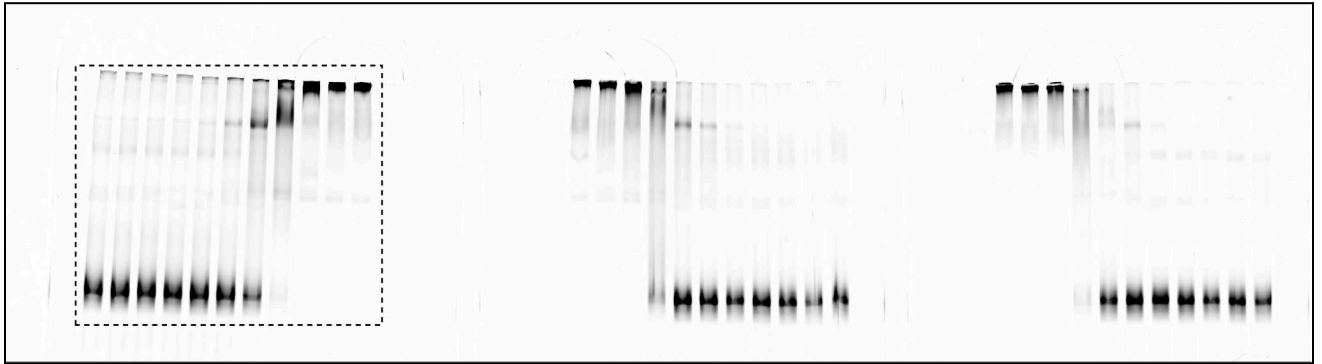
mismatch 19-23; left panel



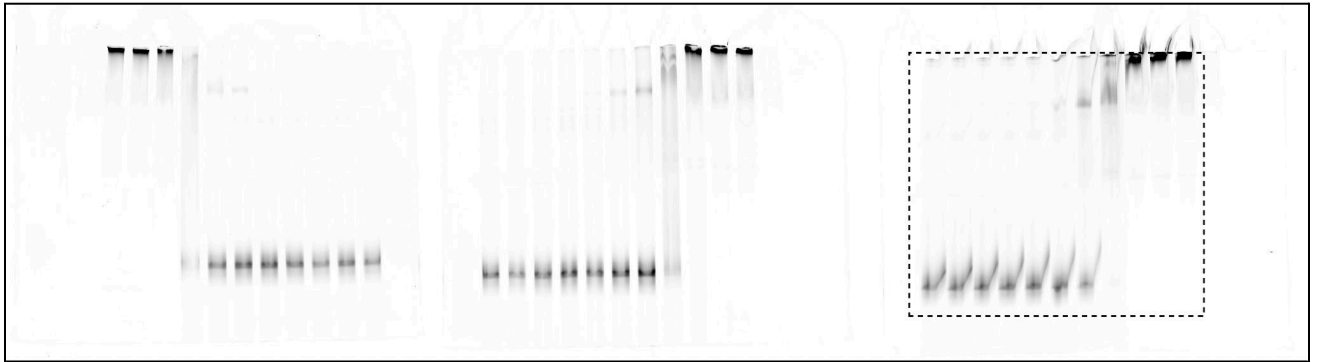
mismatch 19-23; center and right panel



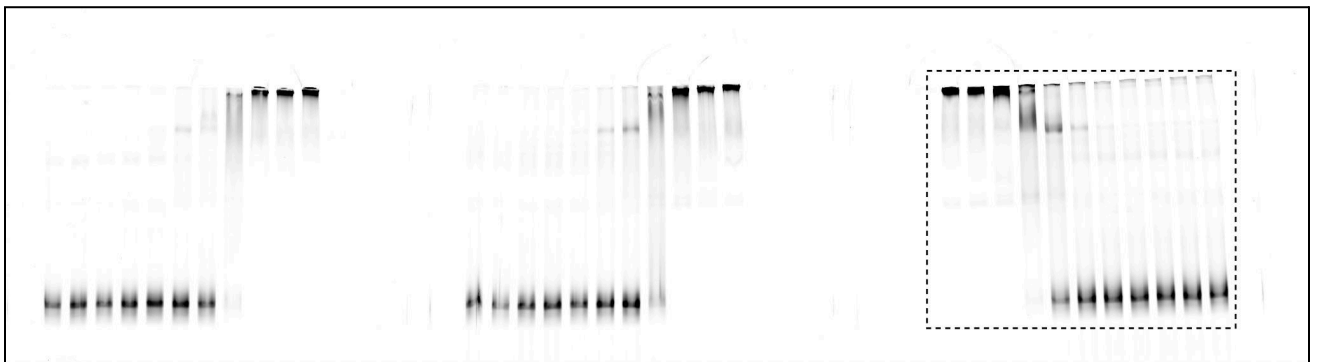
mismatch 25-29: left panel



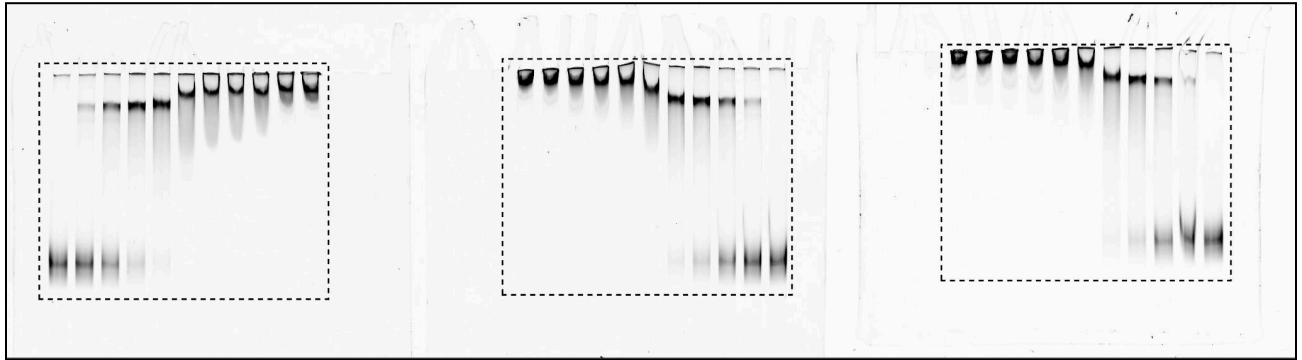
mismatch 25-29: center panel



mismatch 25-29: right panel

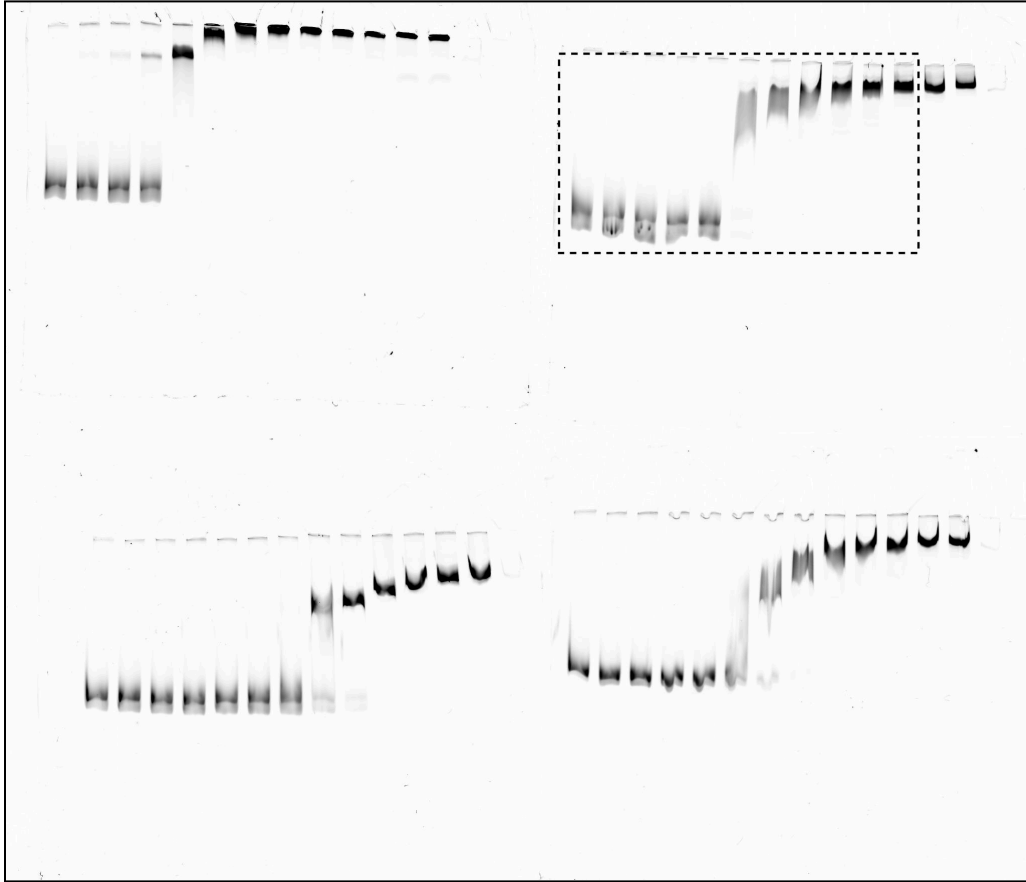


mismatch 31-32: left, center and right panel

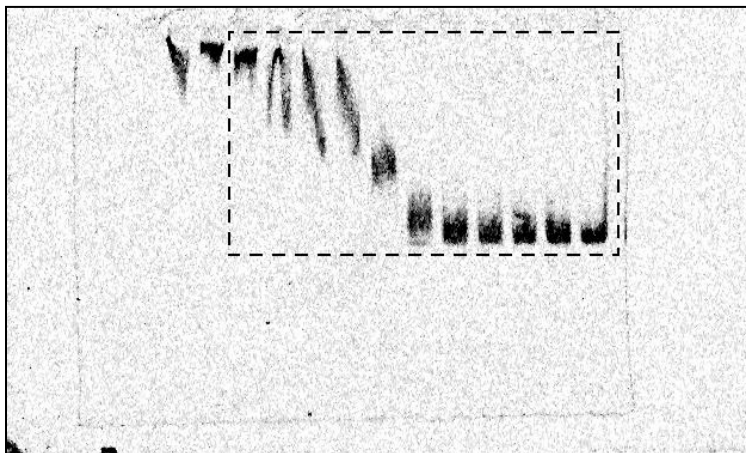


Supplementary Fig. 12a

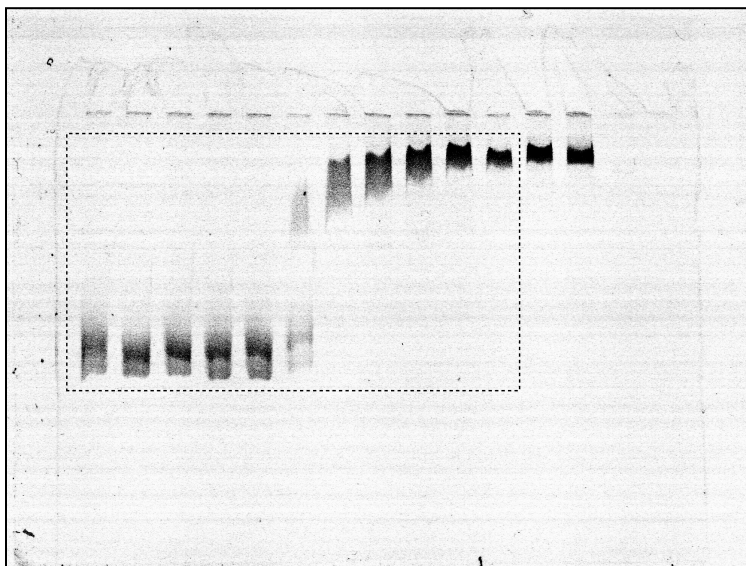
Cas7 Δ 191-208 (GSSG); left panel



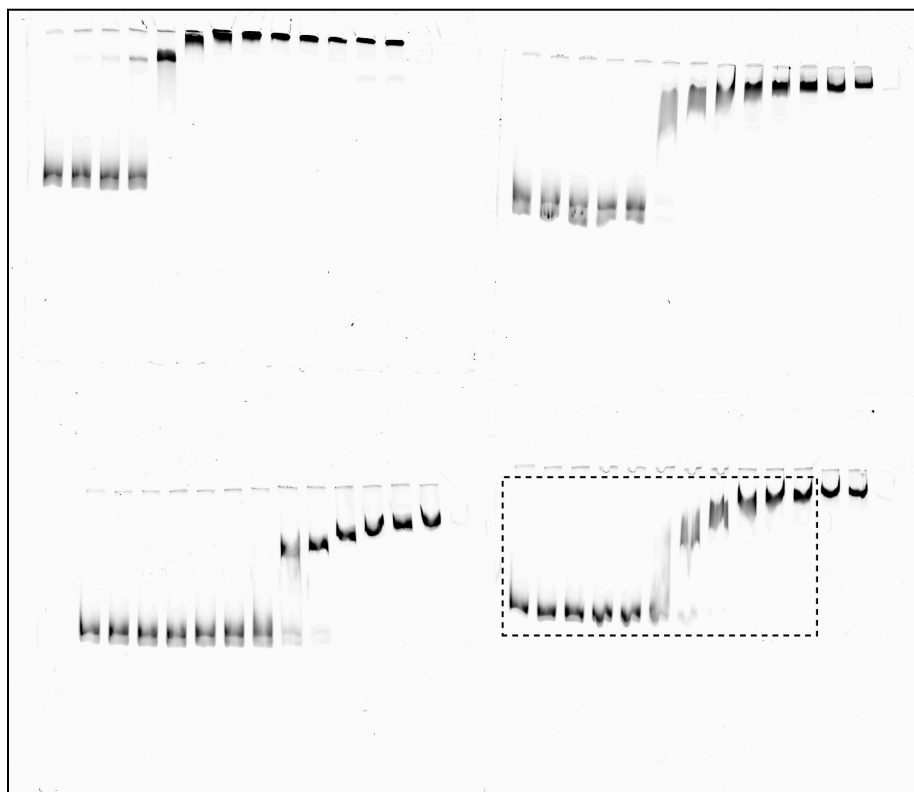
Cas7 Δ 191-208 (GSSG); center panel



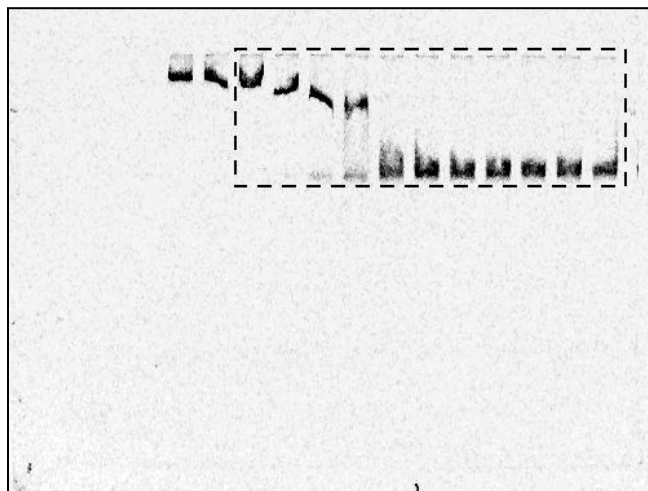
Cas7 Δ 191-208 (GSSG): right panel



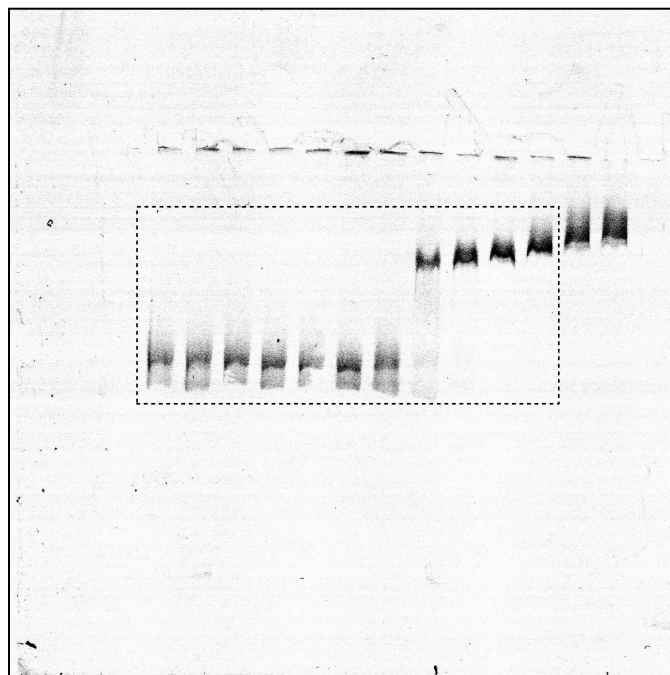
Cas7 Δ 184-216 (GSSG): left panel



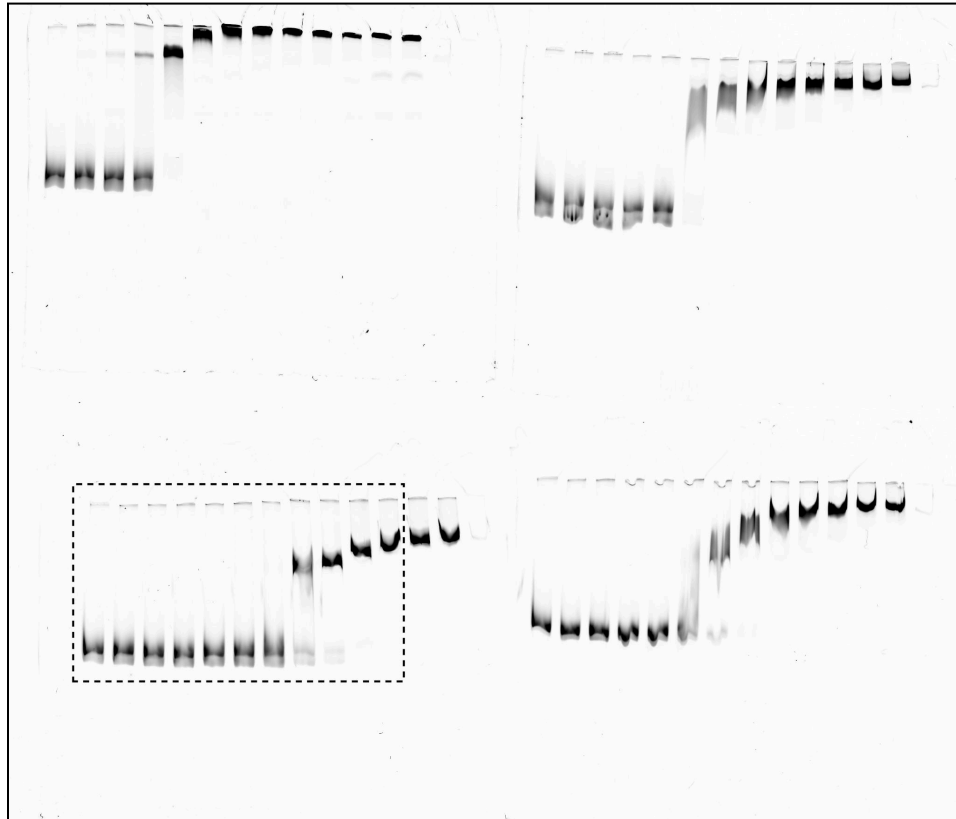
Cas7 Δ 184-216 (GSSG): center panel



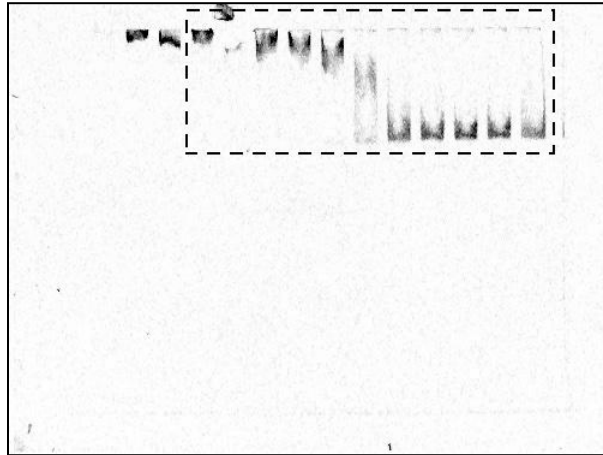
Cas7 Δ 184-216 (GSSG): right panel



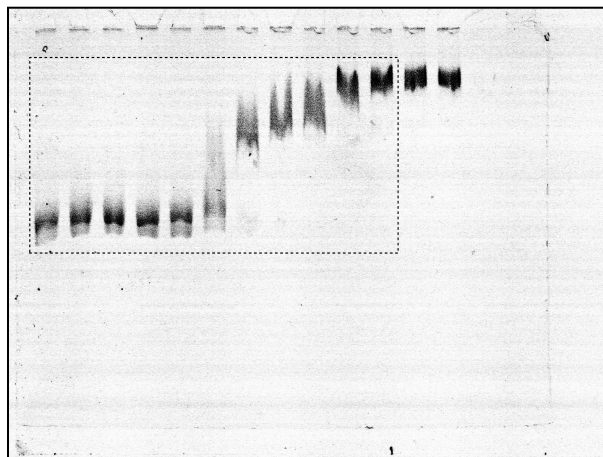
Cas7 Δ 177-224 (GSSG): left panel



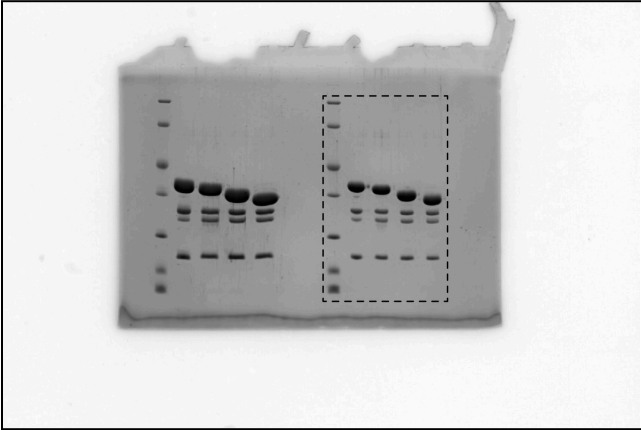
Cas7 Δ 177-224 (GSSG): center panel



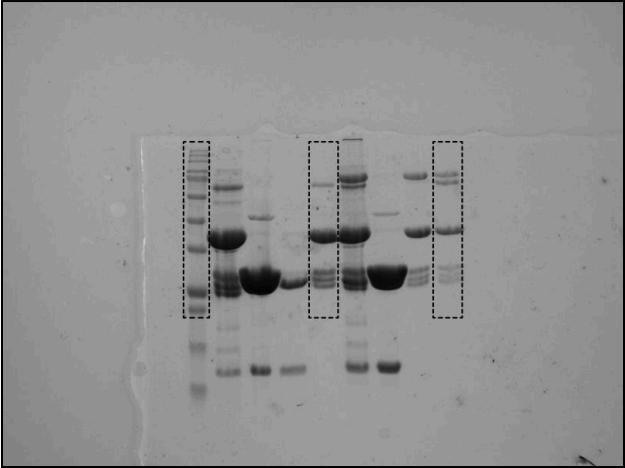
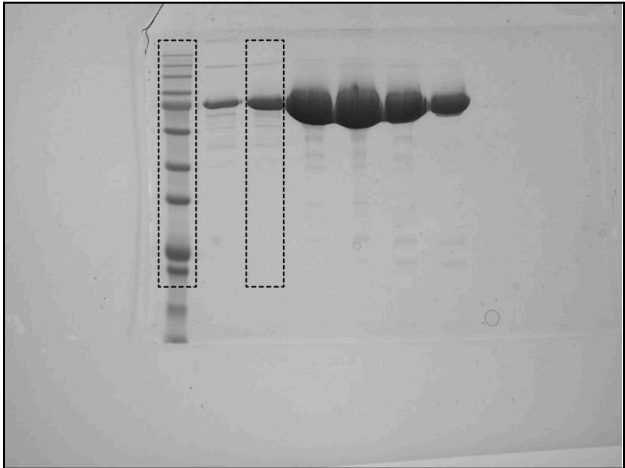
Cas7 Δ 177-224 (GSSG): left panel



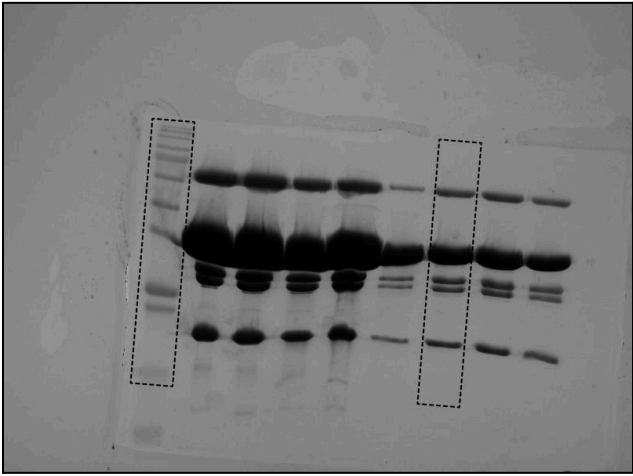
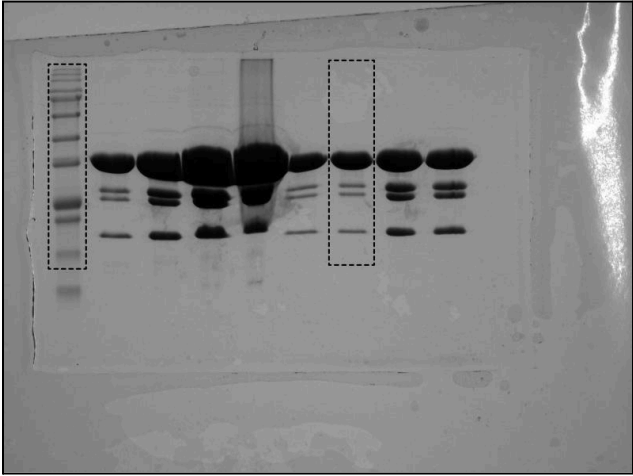
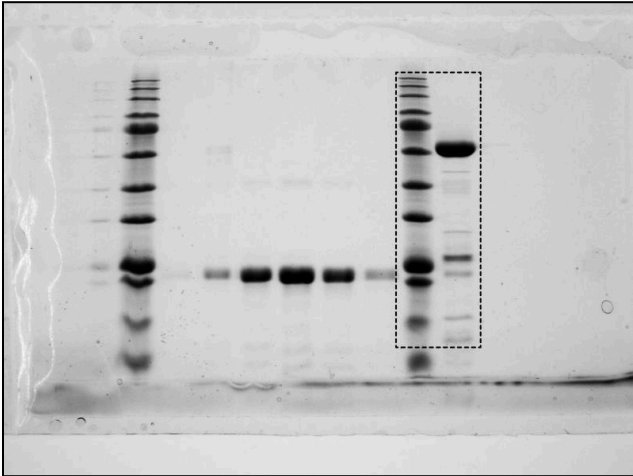
Supplementary Fig. 12b



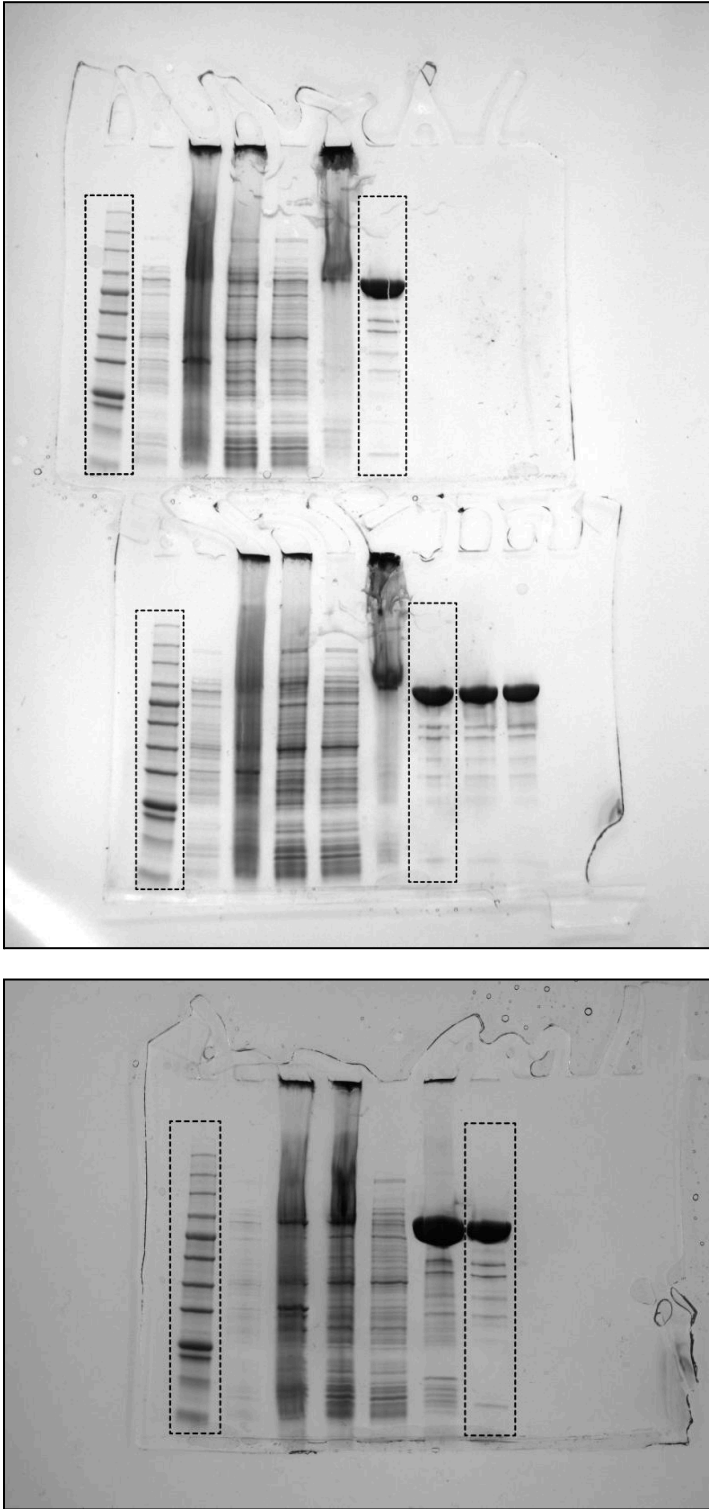
Supplementary Fig. 13a



Supplementary Fig. 13b



Supplementary Fig. 16a



Supplementary Fig. 16b

